SOME STRATOSPHERIC ASPECTS OF MODEL DEVELOPMENT AT ECMWF

A.J. Simmons
European Centre for Medium-Range Weather Forecasts,
Shinfield Park, Reading, UK

1. INTRODUCTION

A number of factors have either motivated past work on the stratosphere at ECMWF or stimulated new interest leading to the holding of this workshop. Foremost is the effect on the tropospheric forecast of the model's representation of the stratosphere, either directly or through data assimilation. In addition, there is a significant user interest in the stratospheric analyses and forecasts produced by ECMWF and other NWP centres. A better treatment of the stratosphere is needed for the assimilation of satellite radiance data, and there is the prospect of improved stratospheric wind analyses through variational assimilation of ozone data. Extreme winds are found in the stratospheric polar jets (especially over Antarctica), and the numerical formulation of a model close to its top level may determine its overall computational stability.

A recent operational change serves as an example of downward influence of the stratospheric treatment on the tropospheric forecast. Fig. 1 shows the root mean square error of the 500 hPa height as a function of forecast range for the extratropical Northern Hemisphere, averaged over two sets of forecasts for the period 27 October to 3 November 1993. The dashed line denotes the (control) operational forecasts and the solid line represents forecasts from new analyses in which radiosonde height biases were corrected. The corrections were made predominantly in the stratosphere, over North America and China. In Fig. 1, no impact is seen on the 500 hPa forecast until beyond day 5, when correction of the radiosonde height biases causes a small mean reduction in forecast error for these eight cases. The correction scheme was subsequently introduced operationally.

Routine objective verification of forecasts shows a substantial improvement in the quality of the stratospheric forecasts since operational forecasting began at ECMWF. Fig. 2 presents anomaly correlations of height calculated over the extratropical Northern Hemisphere for the 200 hPa and 50 hPa levels, for 3-, 5-, 7- and 10-day forecasts. 12-month moving averages of monthly-mean values are plotted for the period from 1981 to the present. A fairly steady improvement is seen at 200 hPa, and an apparently much larger one at 50 hPa. Particularly evident is the increase in anomaly correlation at 50 hPa during 1986. This year saw an increase in vertical resolution in the model stratosphere in May and the introduction of a parametrization of gravity-wave drag in July. Improvement at 50 hPa is also clear in other objective scores; tendency correlations and root mean square errors are presented in Fig. 3. These scores do not, however, show an especially large improvement for 1986.

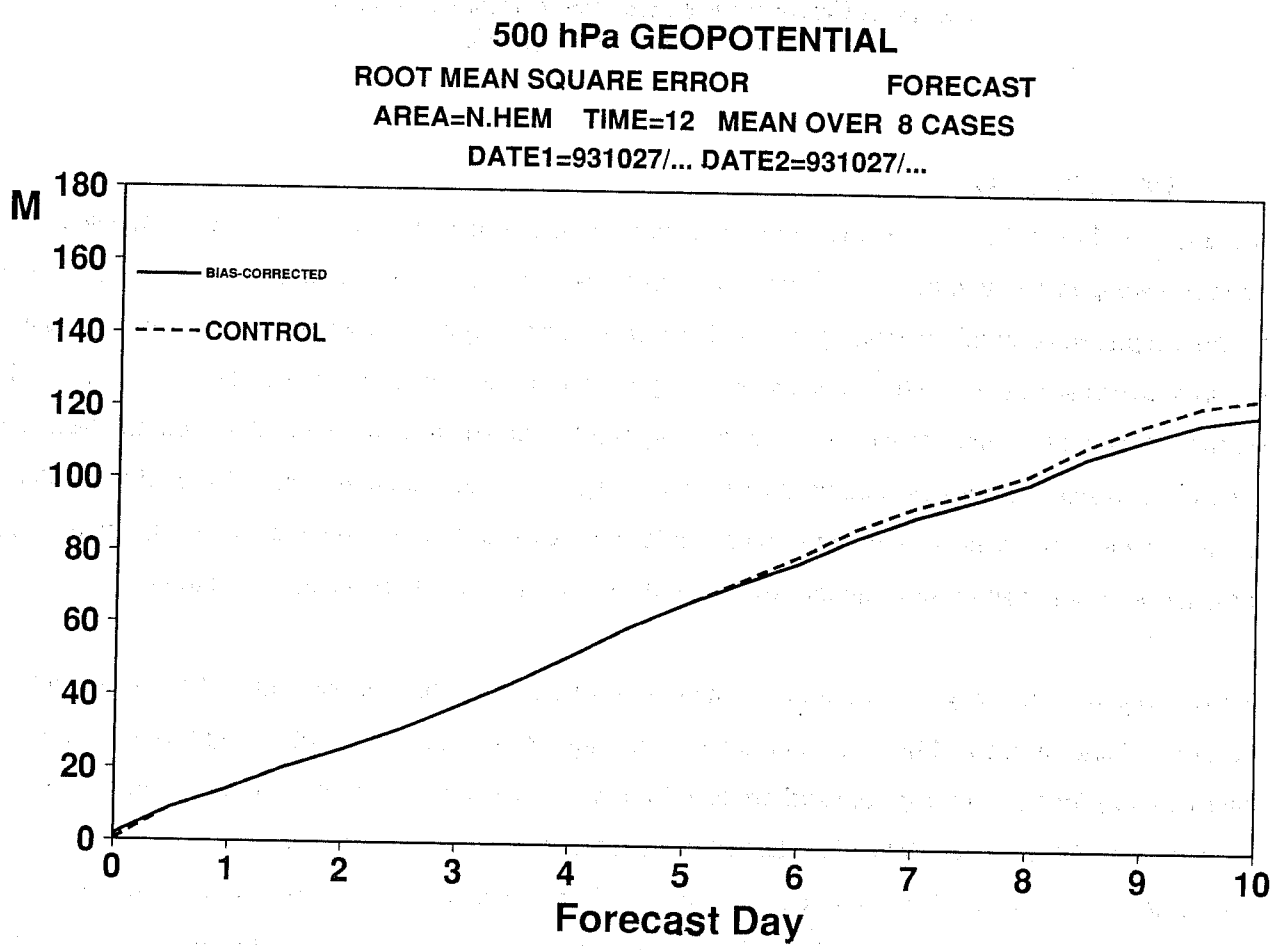

Fig. 1 Root mean square error of the 500 hPa height field for the extratropical Northern Hemisphere averaged over 8 cases. The dashed line denotes the control forecasts and the solid line the forecasts from a data assimilation trial in which radiosonde biases were corrected.

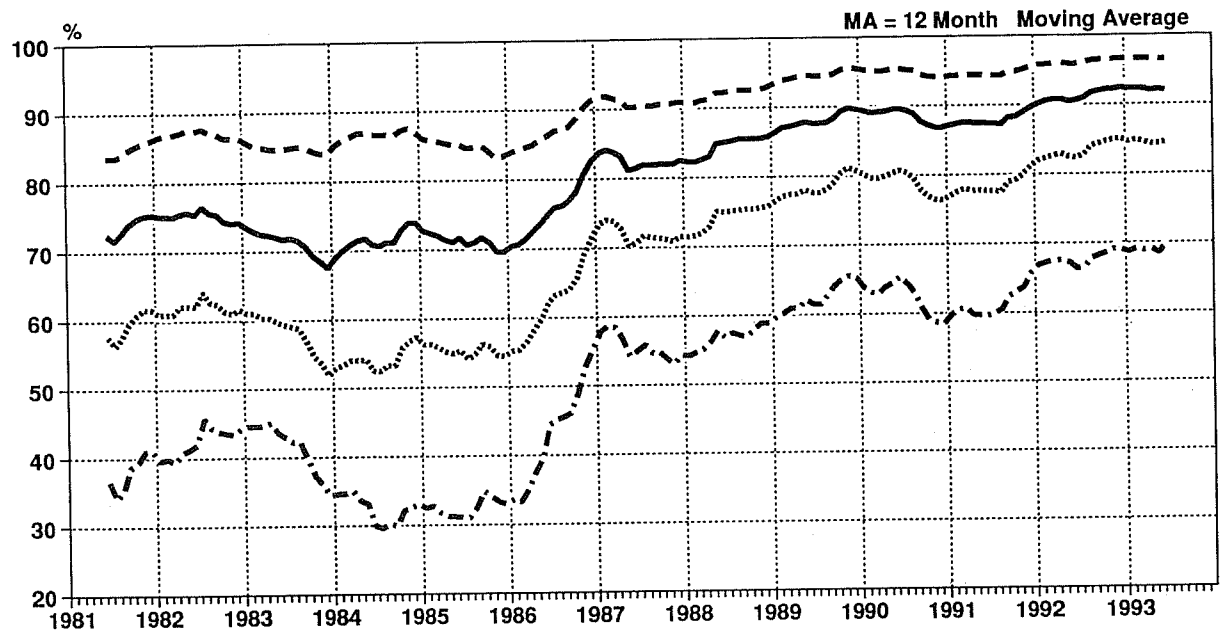

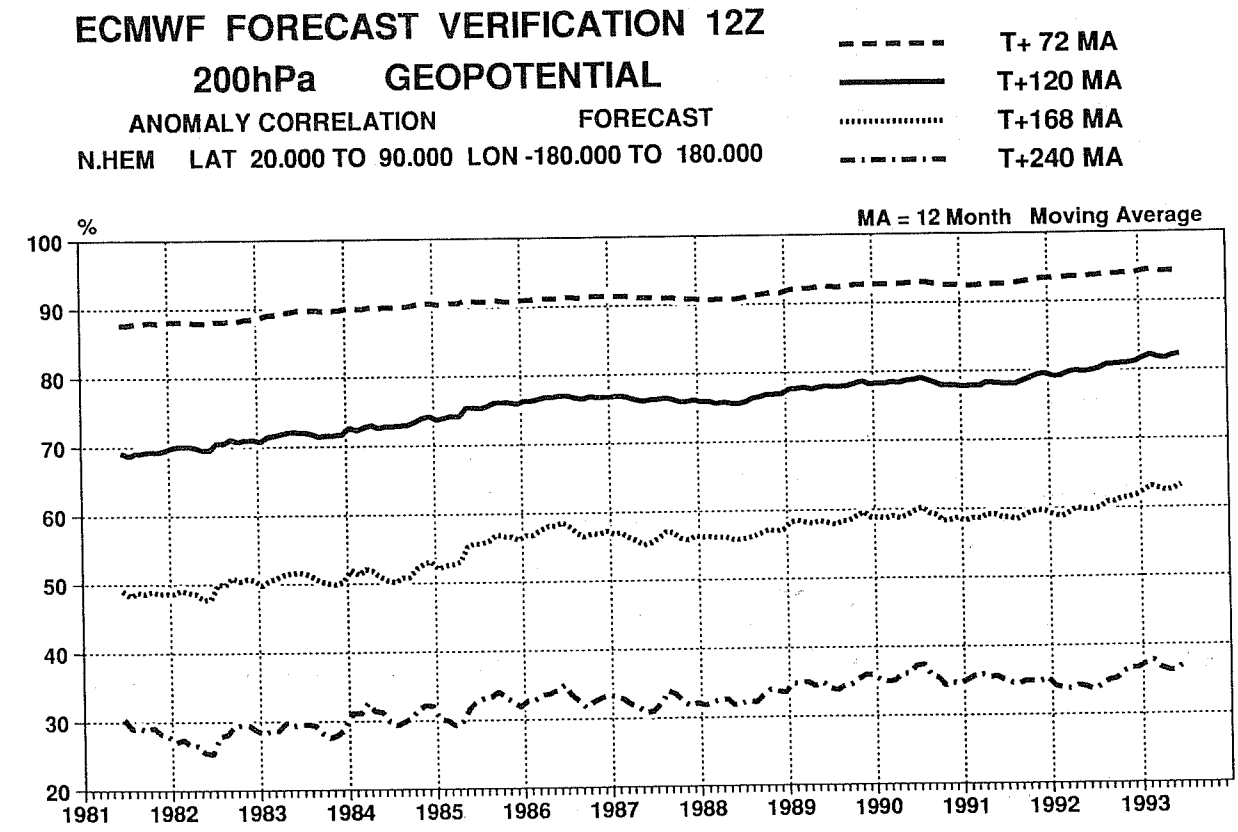

Fig. 2 Time series of anomaly correlations of 50 hPa (upper) and 200 hPa (lower) height for the extratropical Northern Hemisphere, based on operational 3-, 5-, 7- and 10-day forecasts from 1981 to 1993.

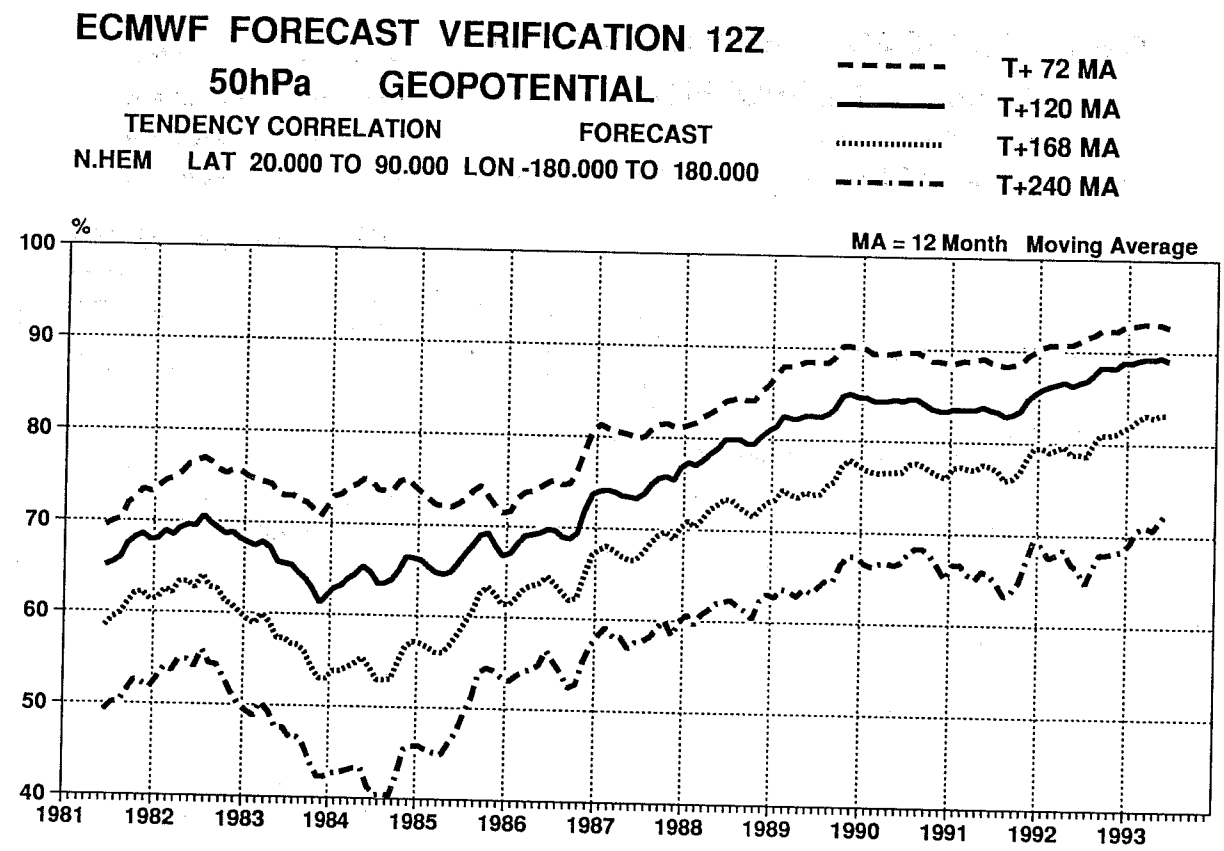

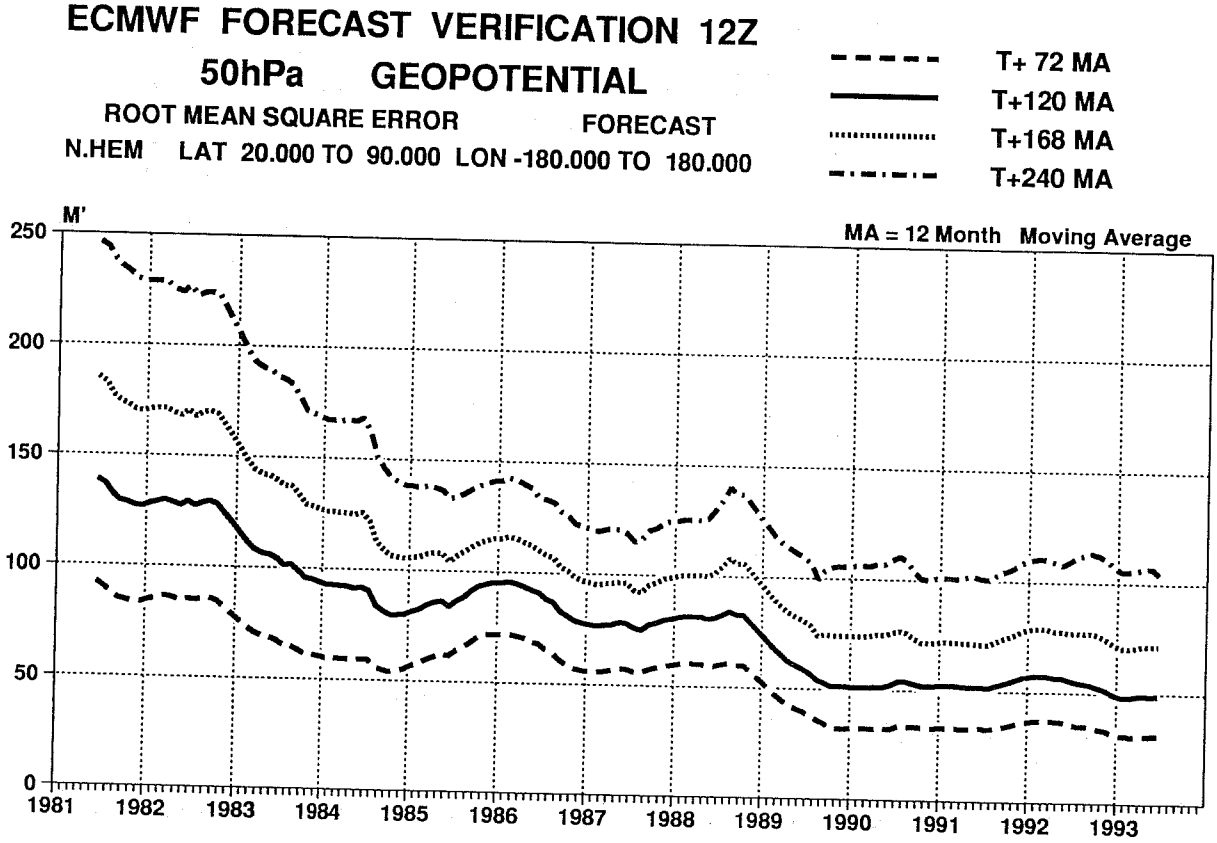

Fig. 3 Time series of tendency correlations (upper) and root mean square errors (lower) of 200 hPa height for the extratropical Northern Hemisphere, based on operational 3-, 5-, 7- and 10-day forecasts from 1981 to 1993.

In the remainder of this paper, we present an account of some of the areas of model development that have been addressed over the past 10 or more years at ECMWF, and that relate particularly to the stratosphere. First, we discuss the hybrid vertical coordinate in operational use since the introduction of the spectral model in April 1983. This was first employed with a 16-level vertical resolution. Discussion of some aspects of subsequent changes to 19- and then to 31-level resolutions is given in section 3. A number of issues relating to what might be generally termed "noise" in the model stratosphere are presented in section 4. This is followed by sections containing limited discussions of the parametrization of gravity-wave drag and the sensitivity to numerical formulation. Section 7 contains early results from an ongoing study to assess the impact of a further increase in stratospheric resolution.

2. HYBRID VERTICAL COORDINATE

The hybrid vertical coordinate used operationally at ECMWF is a terrain-following, sigma coordinate close to the ground, but is a pressure coordinate near the top of the model. A coordinate of this type was in fact first used by groups whose principal interest was in stratospheric modelling (*Schlesinger and Mintz*, 1979; *Fels et al.*, 1980). The form of coordinate developed at ECMWF (*Simmons and Burridge*, 1981; *Simmons and Strüfing*, 1983) differed from that adopted earlier in that the change from a terrain-following to a pressure coordinate occurs smoothly rather than abruptly. This is controlled by a smooth variation with level number k of parameters $A_{k+1/2}$ and $B_{k+1/2}$, which determine the pressures, $p_{k+1/2}$, of the half model-levels which define layer interfaces:

$$p_{k+1/2} = A_{k+1/2} + B_{k+1/2}\, p_s$$

where p_s is surface pressure. Full-level pressures, p_k, where the main model variables are held, are given by:

$$p_k = 0.5\ (\ p_{k+1/2} + p_{k-1/2}\ )$$

Illustrations of the distributions of full-level pressures are given in Fig. 4, for the 16-, 19- and 31-level vertical resolutions that have been used operationally. Coordinate surfaces gradually flatten with increasing height, and are close to surfaces of constant pressure throughout the stratosphere.

Some general arguments and specific results in favour of use of this coordinate (including some successful forecasts of stratospheric warmings) have been given by *Simmons and Burridge* (1981) and *Simmons and Strüfing* (1983), and will not be repeated here. We have, however, recently carried out a new set of comparisons of sigma- and hybrid-coordinate forecasts, to test whether the hybrid coordinate continues to work satisfactorily compared to the sigma coordinate when a semi-Lagrangian advection scheme is used. Such a scheme was introduced operationally at ECMWF in September 1991 along with an increase in horizontal resolution from T106 to T213 and the increase in vertical resolution from 19 to 31 levels (*Ritchie et al.*, 1994).

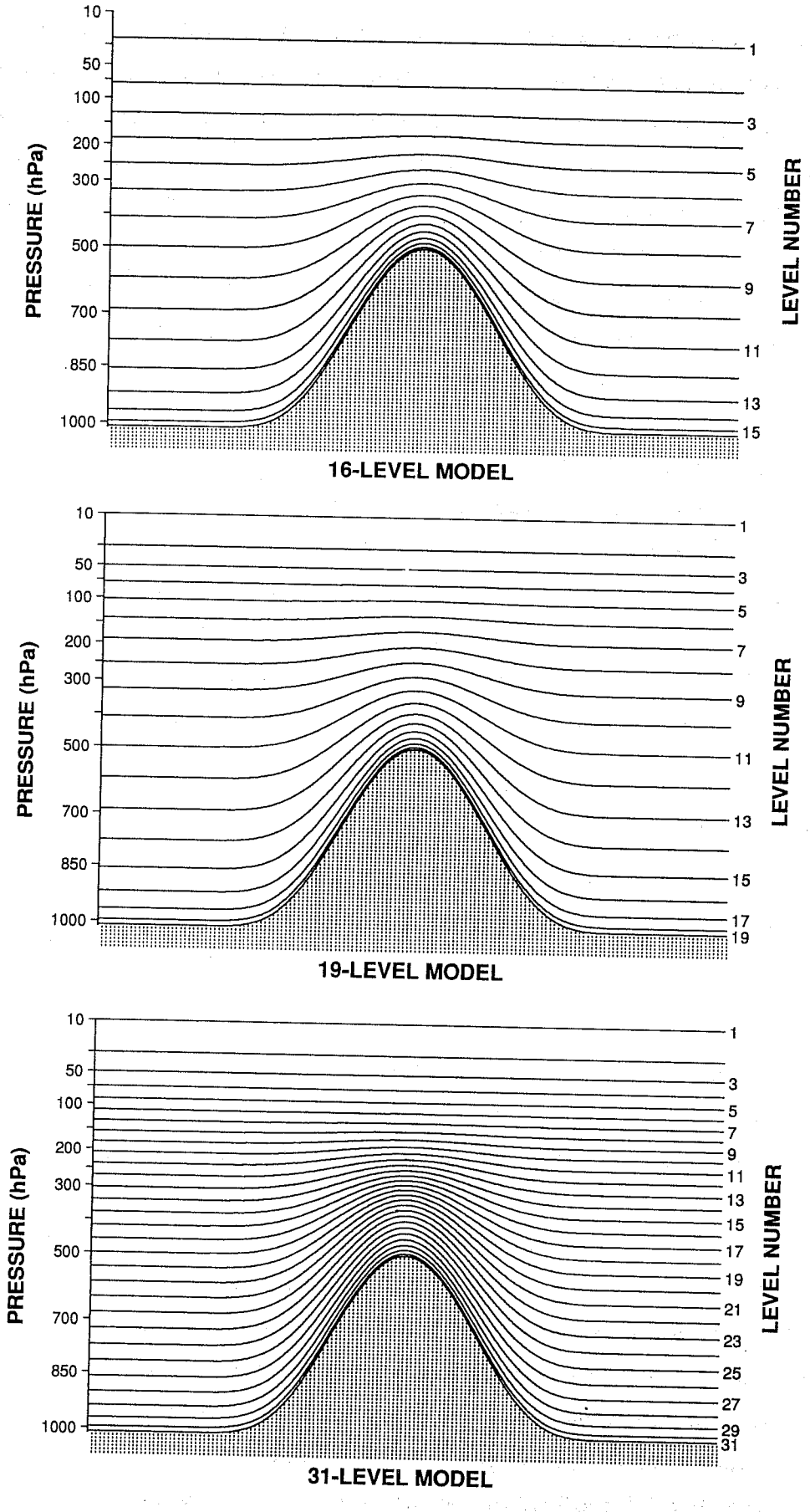

Fig. 4 Distribution of full model levels for operational 16-, 19- and 31-level vertical resolutions.

The comparison of sigma- and hybrid-coordinate forecasts was carried out at the current operational resolution for a set of 12 cases, from the 15th of each month for a year starting 15 October 1991. Sigma levels were chosen to coincide with hybrid levels for the reference surface pressure of 1013.25 hPa. No data assimilation was carried out, so initial analysis fields produced on the hybrid model levels had to be extrapolated above the 10 hPa topmost level in places as part of the construction of sigma-coordinate fields. This may have been to the detriment of the sigma-coordinate results, but the converse is also possible, since one of the advantages of the hybrid coordinate is for data assimilation, in that model levels can be chosen which coincide everywhere with the standard stratospheric pressure levels at which observational data are available.

Objective verification showed that the two coordinates produce very similar tropospheric forecasts, as can be seen in the scatter plots of 500 hPa height anomaly correlations presented in the upper panels of Fig. 5 for days 5 and 7 of the forecast range. At stratospheric levels, however, there is an almost systematic advantage in favour of the hybrid coordinate, as illustrated by the 50 hPa height and 100 hPa temperature anomaly correlations for day 7 also included in Fig. 5. Moreover, stratospheric maps are notably noisier for the sigma coordinate, as in the sample 10 hPa maps shown in Fig. 6. Acknowledging the possible bias in the experimental set-up, the results of these experiments confirm our earlier conclusion (*Simmons et al.*, 1989) that the advantages of using the hybrid coordinate outweigh the disadvantages of a somewhat more complicated formulation and code, and slightly higher computational cost.

3. 16- , 19- AND 31-LEVEL VERTICAL RESOLUTIONS

The principal motivation for the change from the 16-level to the 19-level resolution (Fig. 4) came from problems with the operational startospheric analyses produced using the 16-level model. Because of the limited stratospheric resolution of this model, it was used in data assimilation to provide first-guess information only up to 50 hPa, and the procedures used to provide an analysis at higher levels proved unsatisfactory (*Simmons et al.*, 1989). The 19-level resolution was designed to remedy the problems by providing a model first guess that could be used directly at all analysis levels.

Some test results indicating the impact of the change in stratospheric resolution on 500 hPa height forecasts are presented in Fig. 7. The first comparison of the 16- and 19-level resolutions in data assimilation was for the period from 14 to 26 February 1985 using T63 horizontal resolution. Six forecasts were carried out, each separated by two days. A second assimilation was carried out using T106 resolution from 24 to 30 March 1986, and a further three forecasts were run. Anomaly correlations of the 500 hPa height field are shown in the upper panel of Fig. 7, averaged over the nine forecasts run in total. As in the example presented in Fig. 1 there is negligible impact up to day 5, but beyond this range the benefit of the improved

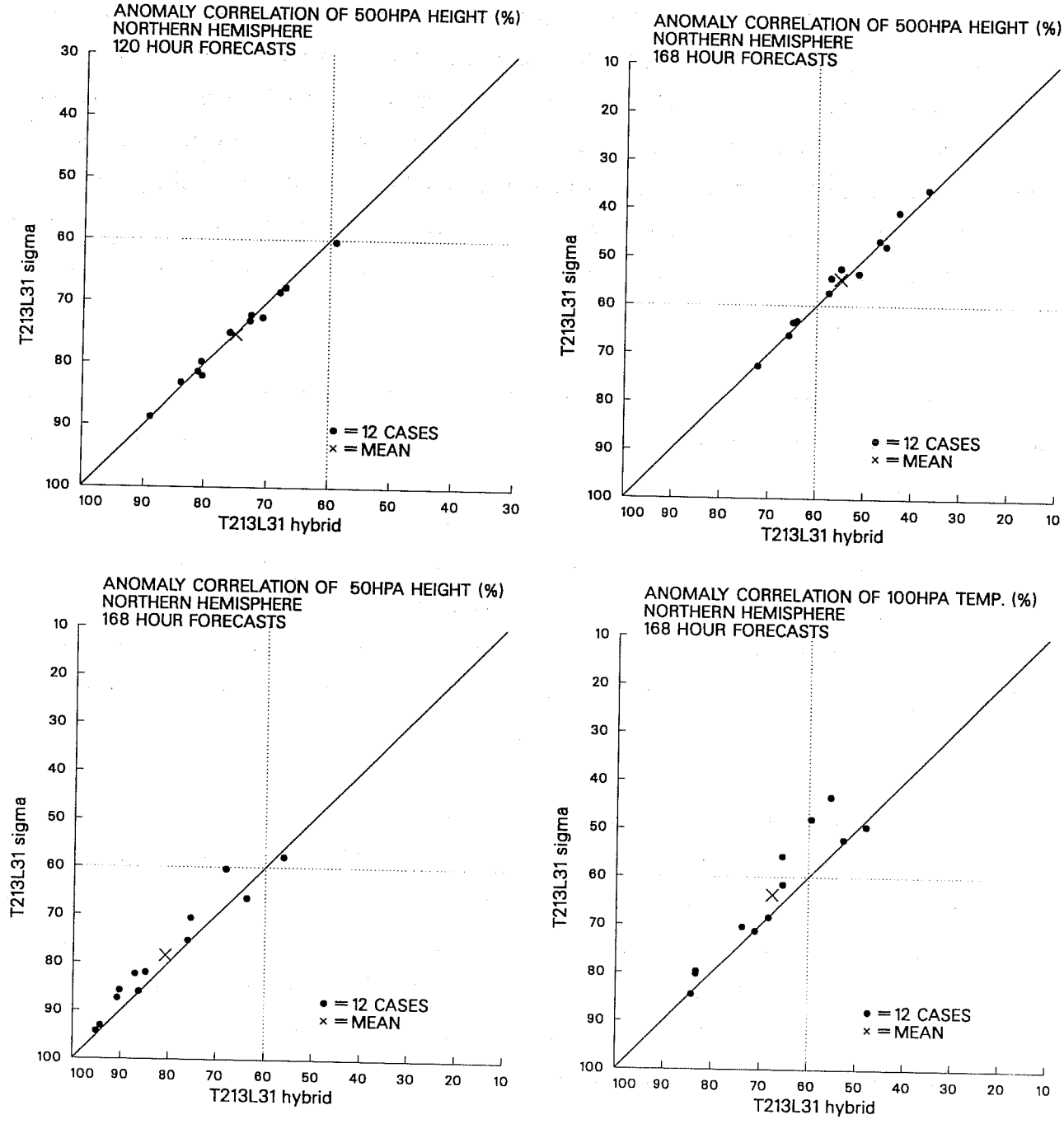

Fig. 5 A selection of scatter plots of anomaly correlations for 12 cases comparing sigma- and hybrid-coordinate forecasts.

Wednesday 15 January 1992 12z ECMWF Forecast t+120 VT: Monday 20 January 1992 12z
10hPa height Hybrid coordinate

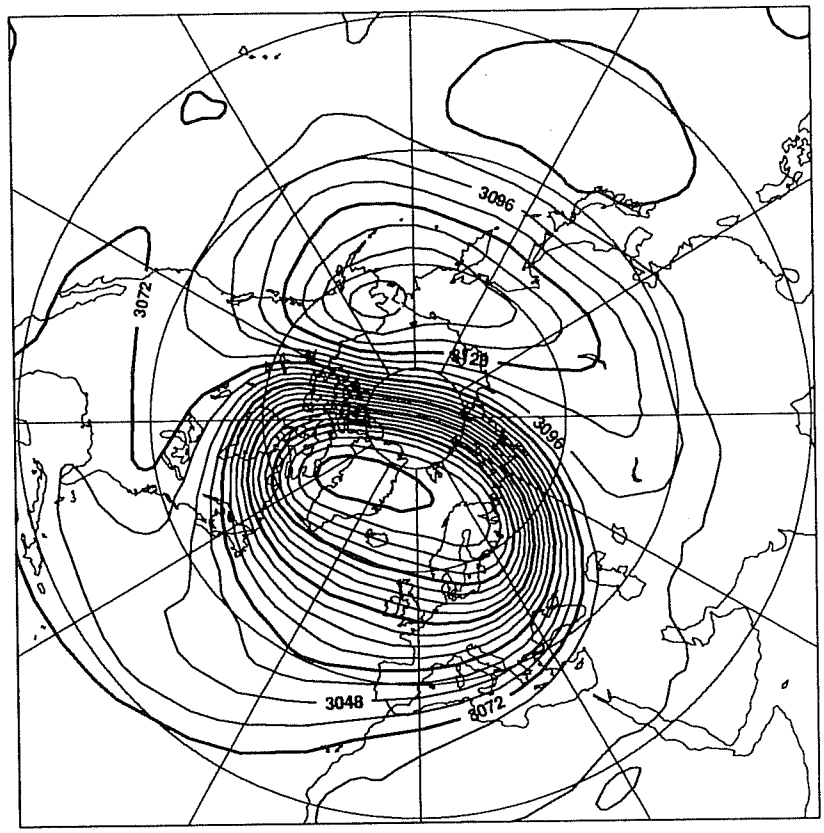

Wednesday 15 January 1992 12z ECMWF Forecast t+120 VT: Monday 20 January 1992 12z
10hPa height Sigma coordinate

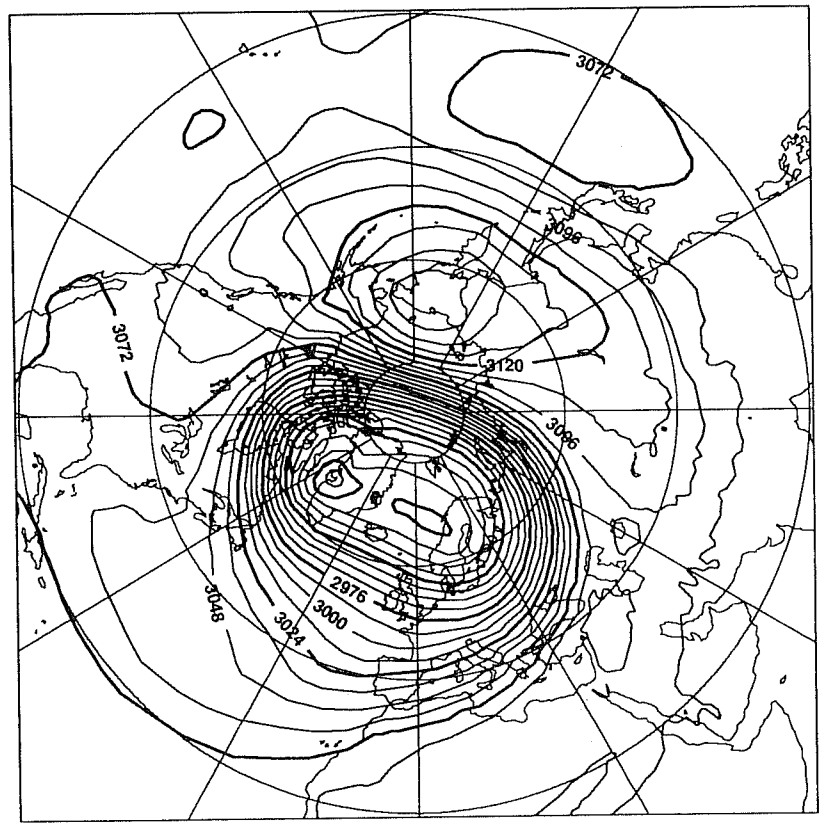

Fig. 6 Day-5 forecasts of 10 hPa height (contour interval 12dam) from 12UTC 15 January 1992, using a hybrid coordinate (upper) and sigma coordinate (lower).

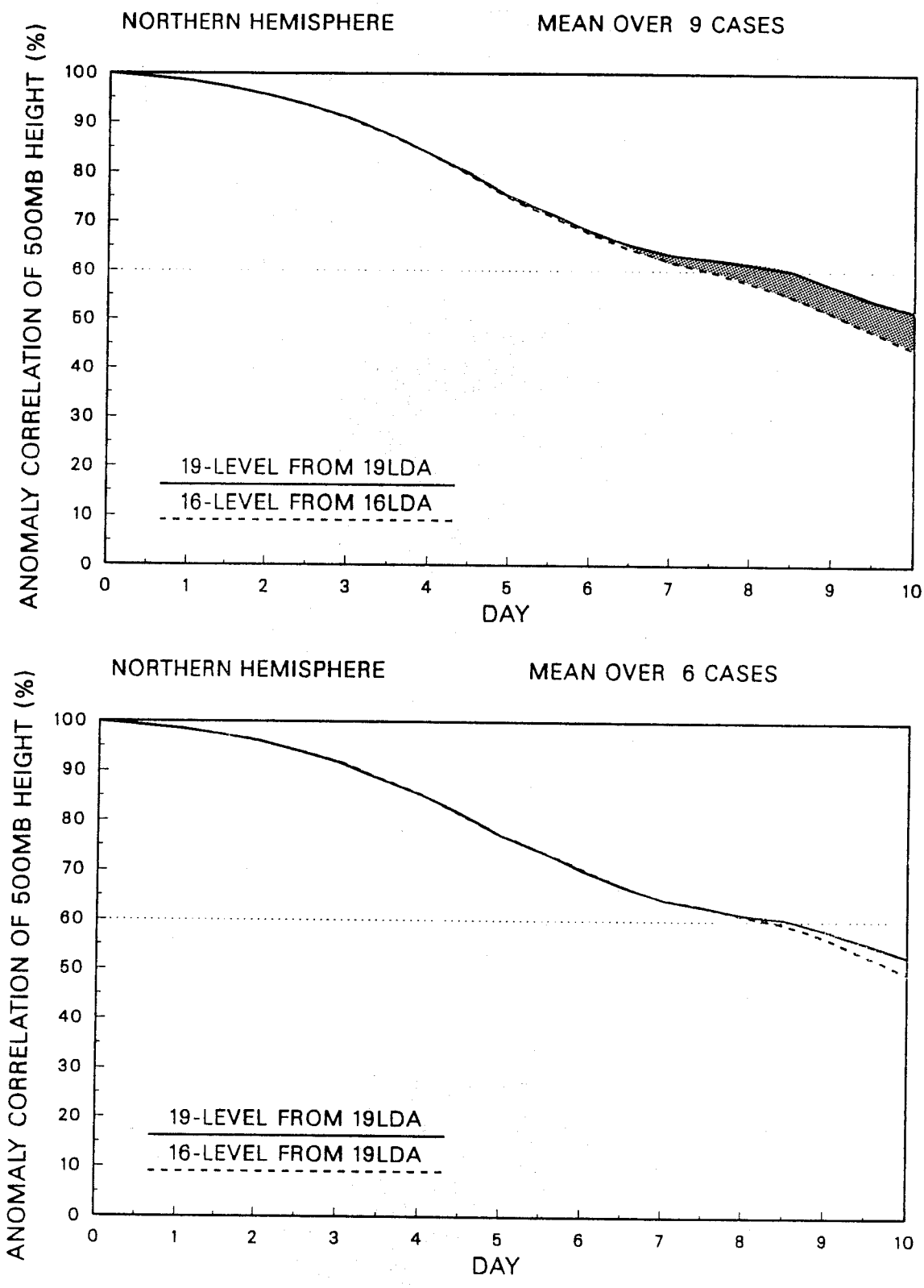

Fig. 7 Mean anomaly correlations of 500 hPa height for the extratropical Northern Hemisphere. The solid lines denote 19-level forecasts and the dashed lines 16-level forecasts. In the upper panel the 16-level forecasts were run from 16-level assimilations, and in the lower panel they were run from interpolated 19-level assimilations.

stratospheric treatment is evident at 500 hPa. A similar result was found when each of the two sets of cases was verified separately.

For the first six cases, the 16-level vertical resolution was also used to run forecasts from initial fields derived by vertical interpolation from the 19-level analyses. The lower panel of Fig. 7 compares the mean anomaly correlations from these six forecasts with those from the six forecasts produced by the complete 19-level system. The similarity of the two sets of results indicates that much, though not all, of the improvement brought about by the 19-level system comes from the improved initial analyses.

Subjective assessment of these forecasts revealed a distinct improvement over Europe in the latter half of the 10-day range. This was found in many individual cases, and shows clearly in ensemble-averaged maps. Fig. 8 presents, from the first period of data assimilation, 6-case average 500 hPa heights for the three sets of day-10 forecasts and for the corresponding verifying analyses. The latter is shown in the upper left panel. Upper right is the mean 19-level forecast from the 19-level assimilation, and lower left the 16-level forecast from the 16-level assimilation. Improvements in the Atlantic jet, the jet split, and the downstream ridge and trough are evident. The lower right panel shows the corresponding mean forecast using the 16-level model from the 19-level analyses. This captures much of the improvement, in agreement with the result of objective assessment.

It must be borne in mind that the experiments discussed above were carried out for just two late-winter periods, and that the impact of the stratospheric analysis or model on the tropospheric forecast is likely to vary significantly with synoptic situation and season. However, running 16-level forecasts from interpolated 19-level operational analyses for cases from the Northern Hemisphere winter of 1986/87, when the stratospheric vortex was substantially disturbed, showed a *larger* impact of enhanced stratospheric resolution in the second half of the forecast range than in the cases presented here. Moreover, a distinct improvement in the winter tropospheric climate of the model, as determined by a series of 90-day integrations at T42 resolution, was found when vertical resolution was increased from 16 to 19 levels (*Simmons*, 1987). This is in agreement with results obtained elsewhere, such as by *Boville* (1984), concerning the sensitivity of tropospheric simulations to the representation of the stratosphere.

The operational change to the 31-level vertical resolution was part of a much larger one involving a major increase in horizontal resolution from T106 to T213 and major changes in numerical formulation, as indicated earlier. A deliberate decision was made not to consider a general increase in stratospheric resolution as part of this change, so the uppermost two levels remained in the same position as before, and there was little change in positioning of other levels above about 100 hPa. The 31-level version does,

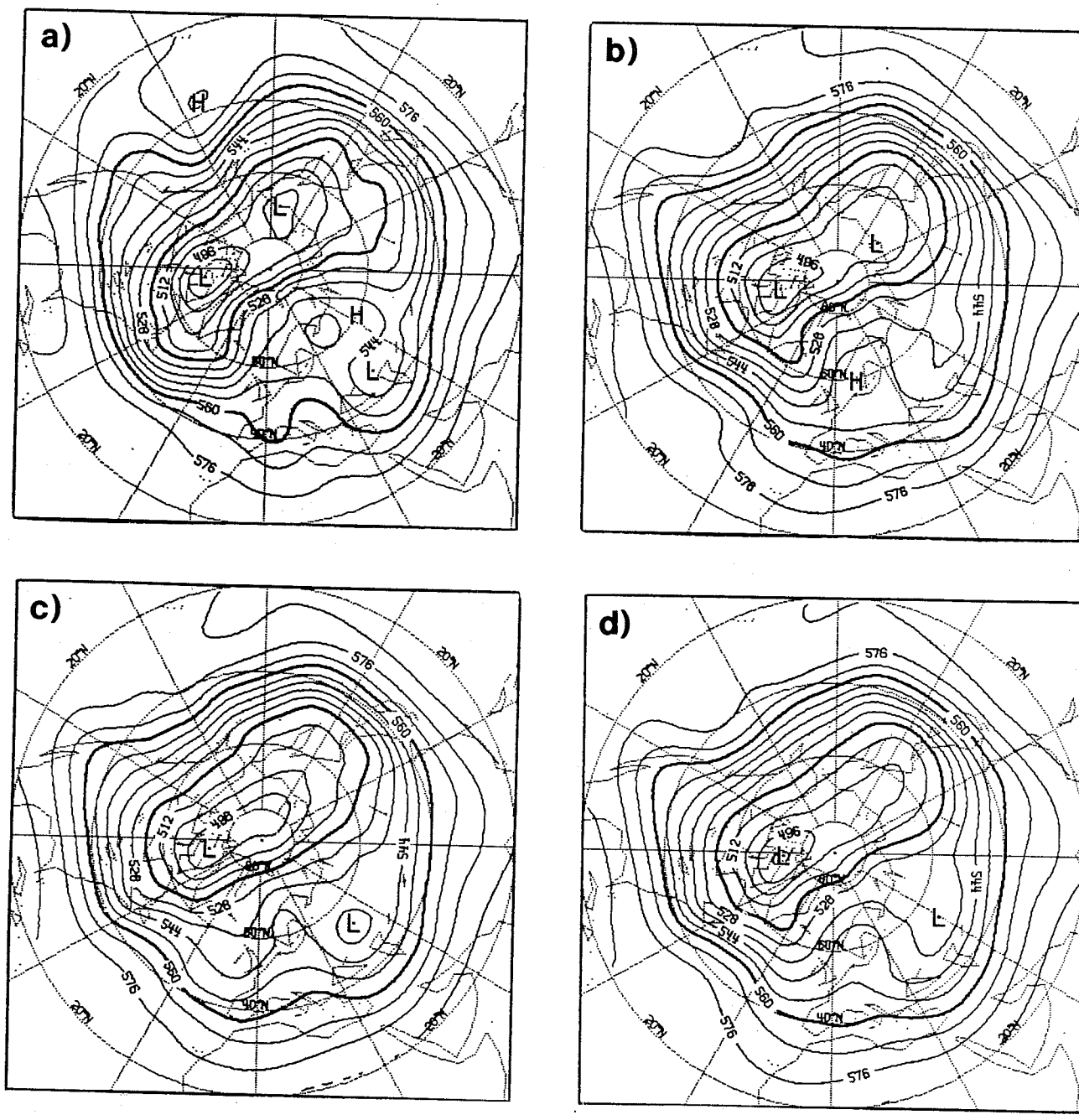

Fig. 8 Ensemble-mean 500 hPa heights (contour interval 8 dam) for a) verifying analyses, b) 19-level day-10 forecasts from the 19-level assimilation, c) 16-level forecasts from the 16-level assimilation, and d) 16-level forecasts from the 19-level assimilation.

however, give a substantially increased resolution at levels typical of the extratropical tropopause and lowermost stratosphere.

The benefit of the 31-level resolution shows up most clearly in the accuracy of the data assimilation at levels around the tropopause. The most recent comparison is a set of three-week assimilations for the period 7 to 27 January 1993 carried out as part of the preparation for the 15-year reanalysis project that has been set up at ECMWF. Here we compare some statistics produced using resolutions T106L19, T106L31 and T213L31 for the assimilating model. Fig. 9 shows the fits of the three analyses to radiosonde data over the extratropical Northern Hemisphere, computed over the full 21-day period. The larger sensitivity is evidently to the change in vertical rather than horizontal resolution, the 31-level analyses giving a much improved fit to radiosondes in the layer from 400 to 100 hPa. This is particularly marked for the mean temperature of the 200-250 hPa and 250-300 hPa layers. Improvement can also be seen clearly for the zonal and meridional wind components, and is discernible for the geopotential height field. These improvements carry over into the fits of the 6-hour first-guess forecasts to the radiosonde data, but diminish in magnitude. Conventional skill scores for the tropospheric forecasts also indicate somewhat better results for the 31-level resolution out to about day 7, though we do not have any indication as to the extent that this is due to better treatment of near-tropopause levels in the data assimilation.

4. STRATOSPHERIC "NOISE" AND HORIZONTAL DIFFUSION

(i) Horizontal diffusion in the model stratosphere

Comparing the data fits of the T213L31 and T106L31 assimilations shown in Fig. 9, we see that the fit at tropospheric levels is a little better with the higher horizontal resolution, as might be expected. However, above about 250 hPa, the fit of the T213 analyses is rather worse than that of the T106 analyses, for variables other than geopotential height. The reasons for this have yet to be investigated fully, but one possibility is that it is a consequence of a higher amount of noise in the T213 analyses, arising from use of a weaker horizontal diffusion in the higher resolution model.

The basic formulation of horizontal diffusion in the ECMWF spectral model is a simple linear 4th-order diffusion applied along the hybrid coordinate surfaces: the diffusive tendency of a variable X is $- K \nabla^4 X$. This form is modified at lower model levels for temperature to avoid a problem of excessive orographic precipitation associated with an unphysical mixing of temperature along sharply sloping terrain-following coordinate surfaces. Also, in versions which use an Eulerian rather than semi-Lagrangian advection scheme, a more highly scale-selective diffusion is applied in addition at levels of strong wind and invariably at uppermost levels. This is a device to increase the timestep that may be safely used (*Simmons et al.*, 1989).

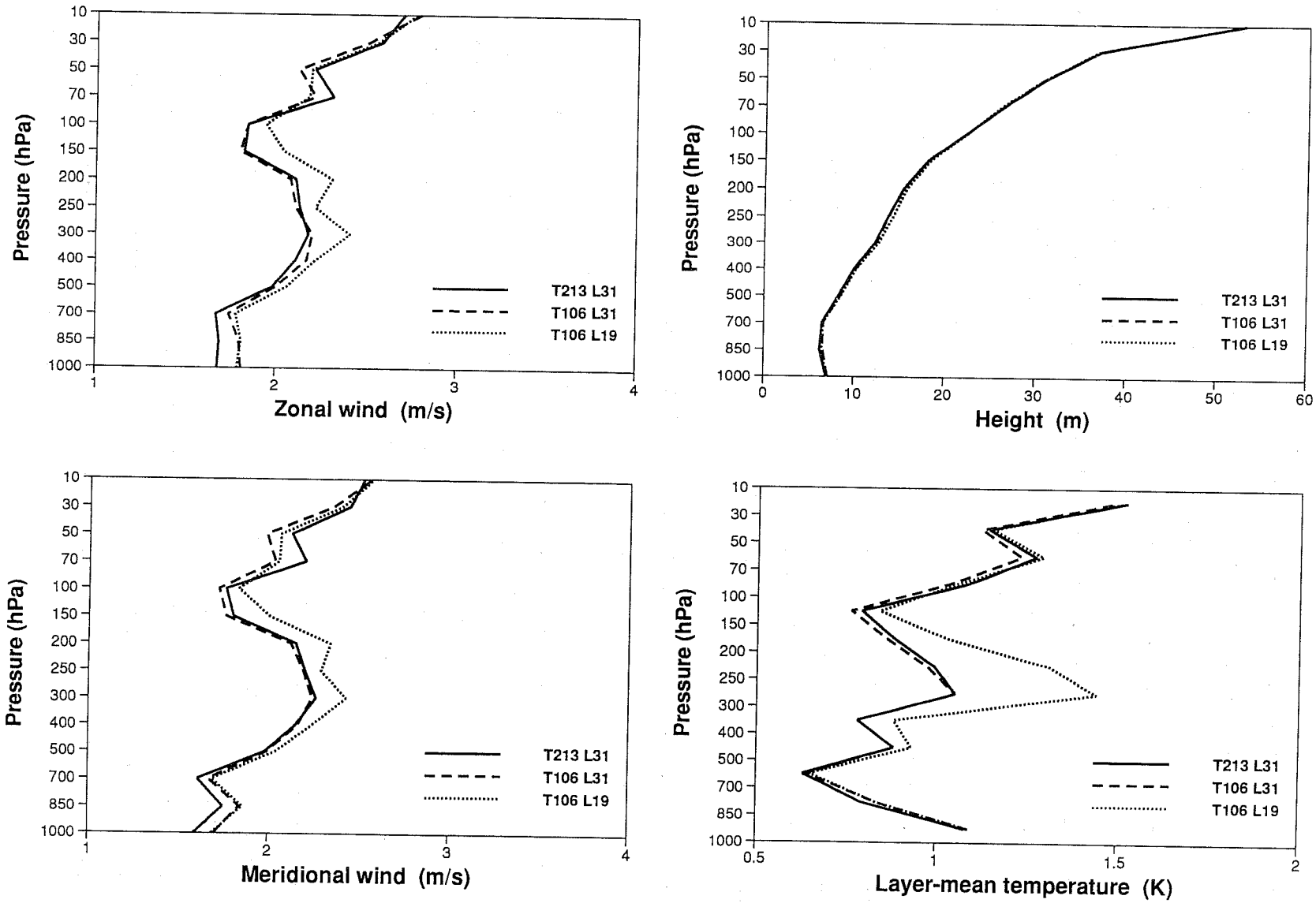

Fig. 9 Root mean square fits of analyses to 12UTC radiosonde data for the extratropical Northern Hemisphere over the period 7 to 27 January 1993, from assimilations using T213L31, T106L31 and T106L19 resolutions.

Apart from the above modifications of the basic 4th-order diffusion, the coefficient K is increased progressively at model levels above 200 hPa. This was first introduced because an increased level of small-scale wave activity was noticed at stratospheric levels when the 19-level resolution was being tested. The increase in diffusion in the stratosphere removes noise in initial fields, and damps vertically propagating small-scale waves that are likely anyway to be mishandled by the model due to limited upper-level resolution and a reflective upper boundary condition. It may also provide a small further aid to computational stability. The precise details of the increase need not concern us here, but to provide an indication, approximate e-folding times of the diffusion applied to total wavenumbers 53 and 106 are presented in Table 1 for the 10, 50, 100 and 200 hPa levels, for the settings chosen for T106L19 and T213L31 resolutions. The values shown for 200 hPa apply to all lower levels.

	n=53		n=106	
	T106 L19	T213 L31	T106 L19	T213 L31
10 hPa	3h	12h	0.2h	0.8h
50 hPa	6h	17h	0.4h	1.1h
100 hPa	1d	1.6d	1.5h	2.4h
200 hPa	2d	8d	3h	12h

Table 1 Approximate e-folding times for (∇^4) diffusion

It is evident from Table 1 that the middle stratosphere is heavily damped in the model, so that the effective horizontal resolution of the model is probably quite substantially lower than the quoted, formal resolution. For T213 horizontal resolution the basic diffusion gives about a factor of four less damping on a given scale, but the way the coefficient is increased with height is such that there is rather more damping around 100 hPa with the 31- than with the 19-level vertical resolution. There is nevertheless appreciably less damping at all levels for the T213L31 than for the T106L19 resolution.

(ii) Potential vorticity fields computed from analyses

Despite the large amount of horizontal diffusion in the model stratosphere, analyzed fields at stratospheric levels still appear to be noisy. This is particularly the case for fields of potential vorticity (PV) derived on isentropic levels from the basic hybrid-level analysis fields. Fig. 10 shows PV on the 450K surface computed from analyses for 18UTC 18 January 1992 and 00UTC 19 January 1992. These are from a trial assimilation using the model version introduced operationally in August 1992; the assimilating model used operationally at the time temporarily used an enhanced diffusion to overcome a problem of computational instability caused by a coding error.

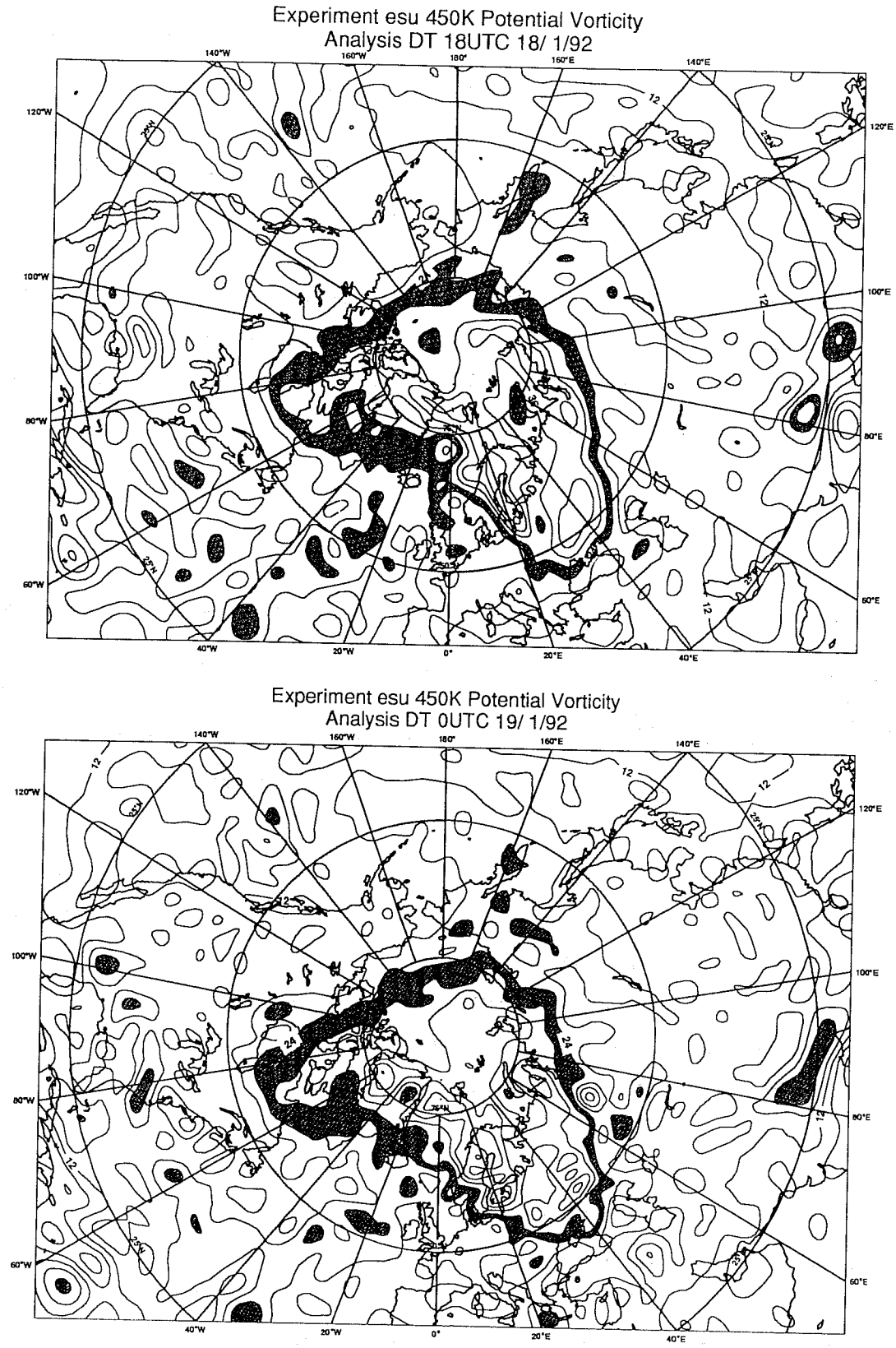

Fig. 10 Potential vorticity on the 450 K isentropic surface computed from analyses for 18UTC 18 January and 00UTC 19 January, 1992. The contour interval is 6×10^{-6} $m^2 s^{-1} K\ kg^{-1}$.

The PV maps shown in Fig. 10 (and virtually any other such map based on stratospheric analyses) show numerous small-scale maxima and minima which disappear rapidly as the forecast proceeds. Some may well be crude attempts to represent genuine small-scale structure such as may occur close to the vortex edge (*Tuck et al.*, 1992), but others appear to be introduced spuriously by the analysis of radiosonde data. Generally, PV maps exhibit more such structures at the main observation times of 00 and 12UTC, when much more radiosonde data is available than at the intermediate times of 06 and 18UTC. In Fig. 10, new maxima appear over the southern USA in the 00UTC analysis, and more wiggles appear at several places around the shaded "vortex edge" region in this analysis.

As a specific example, we examine the dipole structure that appears at 00UTC over the western shore of Hudson Bay. The map in Fig. 11 shows radiosonde observations at 70 hPa over northern North America for this time. The wind observation at the location in question (circled) is substantially weaker than all neighbouring observations and different in direction. The vertical sounding at this station is also plotted in Fig. 11. Wind speeds and directions at levels below 70 hPa are much more coherent with the other observations plotted at 70 hPa, and no measurement is reported higher than 70 hPa from this station. It thus appears that the dipole in PV is associated with an erroneous wind observation close to the top of the balloon's ascent. The subsequent 12UTC sounding shows a similar problem at the top of the ascent, this time at 100 hPa. In this example, quality control procedures appear to have been insufficiently discriminating. More generally, the development of four-dimensional variational assimilation offers the promise of a more dynamically consistent use of data.

For the time being, however, problems remain. A recent example for the Southern Hemisphere is presented in Fig. 12, which contrasts the day-2 forecast of PV on the 475 K surface valid 12UTC 3 November 1993 with the analysis for this time. The case appears to be by no means atypical. The detailed structure visible in the analysis in the vicinity of South America is presumably related to the relatively dense distribution of radiosonde data there (Fig. 13), and the spot at the South Pole is co-located with a radiosonde ascent.

(iii) Computational noise

The strongest winds that normally occur within the domain of the model are found in the Antarctic polar night jet, and over the early years of operational forecasting at ECMWF there were several instances when the operational forecast failed due to computational instability, although in each case it proved possible to complete the forecast by means of a reduced timestep.

During final pre-operational testing of the T213L31 version of the model, a case of noise, though not instability, was encountered at 10 hPa over the edge of Antarctica. The upper plot of Fig. 14 shows isotachs at 10 hPa from the operational day-4 (T106L19) forecast from 28 July 1991, showing winds in excess of

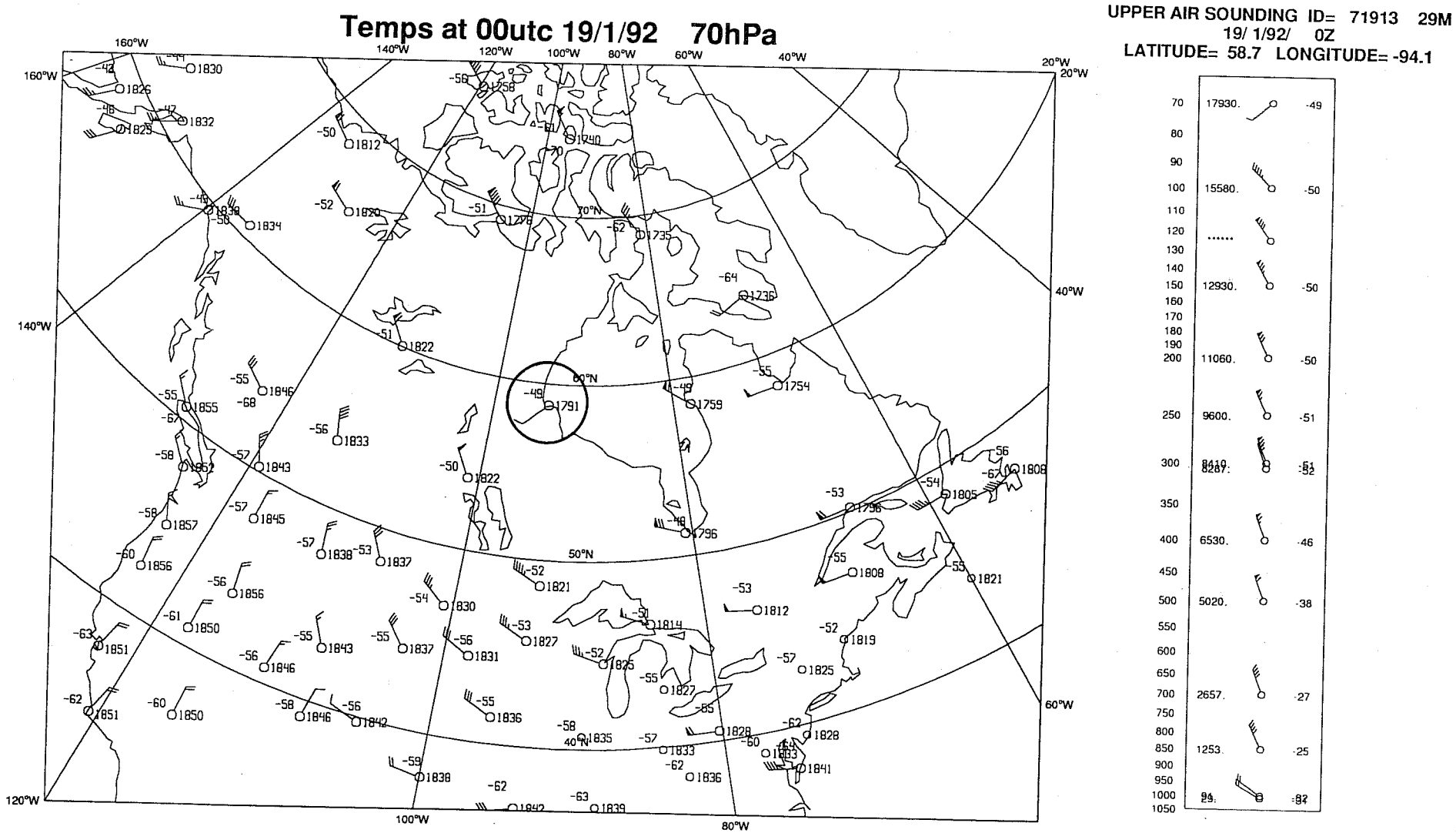

Fig. 11 Radiosonde observations at 70 hPa over North America at 00UTC 19 January 1992 (left), and the vertical sounding at the station discussed in the text (right).

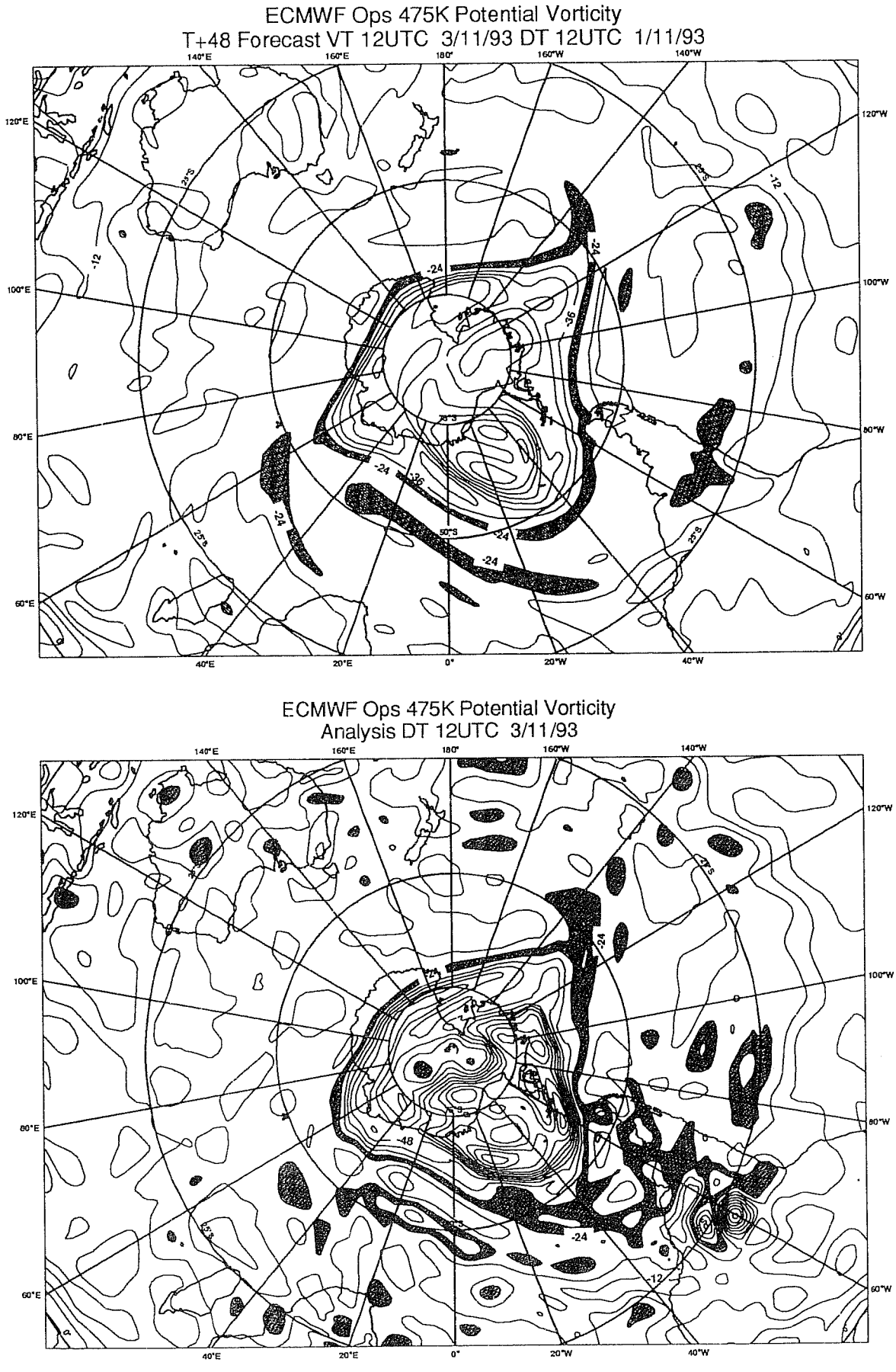

Fig. 12 Potential vorticity on the 475 K surface computed from the day-2 forecast valid 12UTC 3 November 1993 (upper), and from the verifying analysis (lower).

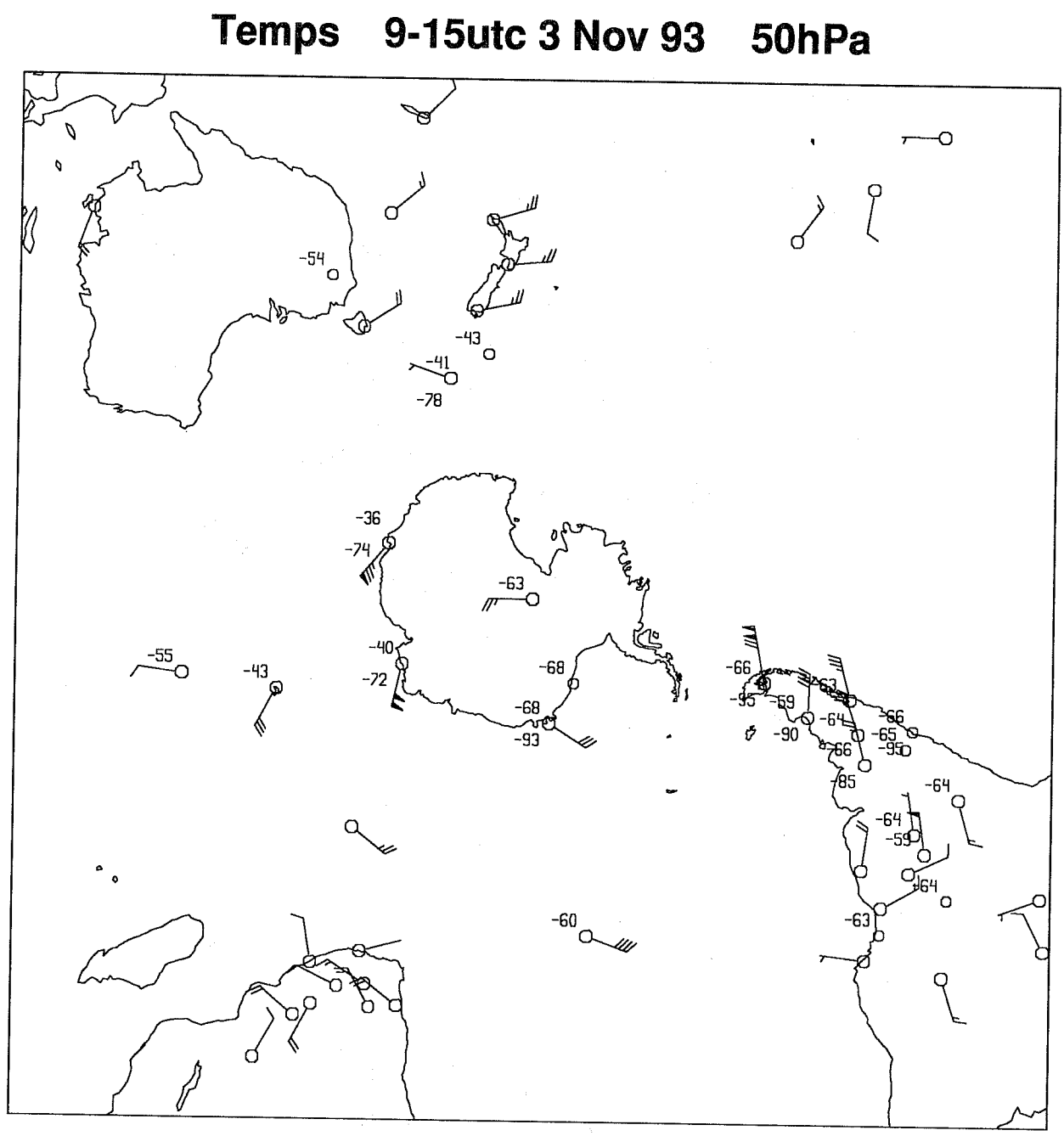

Fig. 13 Radiosonde observations at 50 hPa over the Southern Hemisphere at 12UTC 3 November 1993.

Sunday 28 July 1991 12z ECMWF Forecast t+ 96 VT: Thursday 1 August 1991 12z
Level 1 wind T106 L19

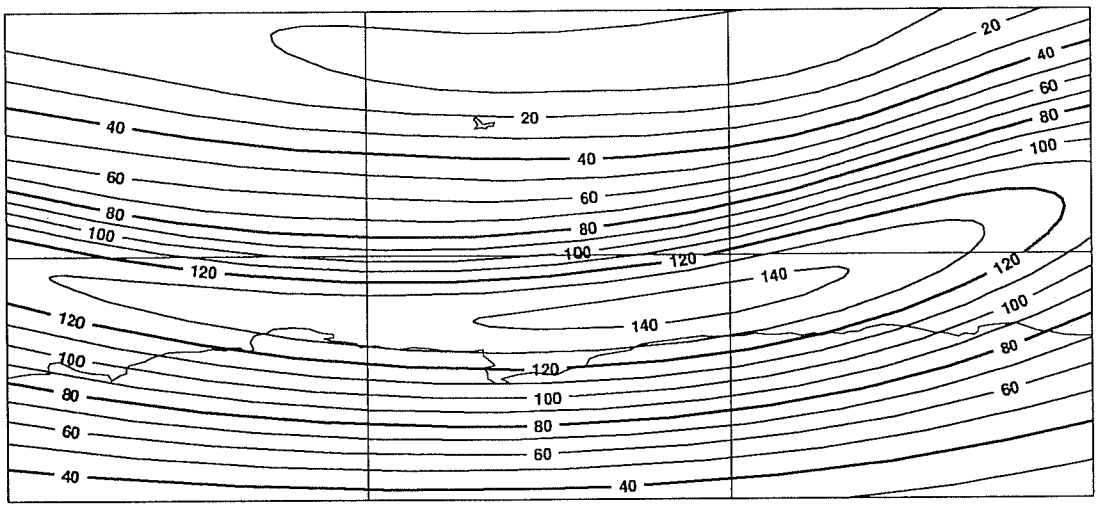

Sunday 28 July 1991 12z ECMWF Forecast t+ 96 VT: Thursday 1 August 1991 12z
Level 1 wind T213 L31

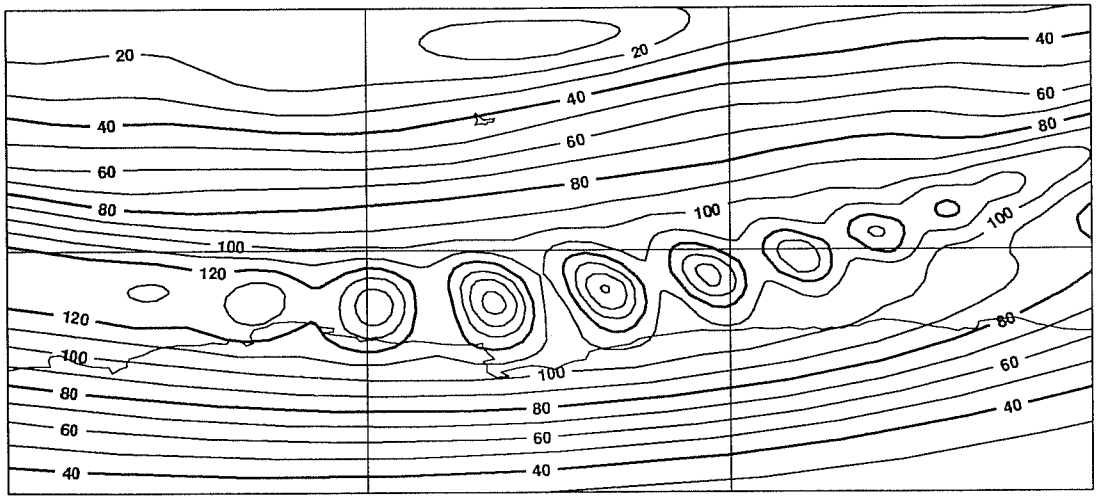

Sunday 28 July 1991 12z ECMWF Forecast t+ 96 VT: Thursday 1 August 1991 12z
Level 1 wind T213 L31 with enhanced diffusion

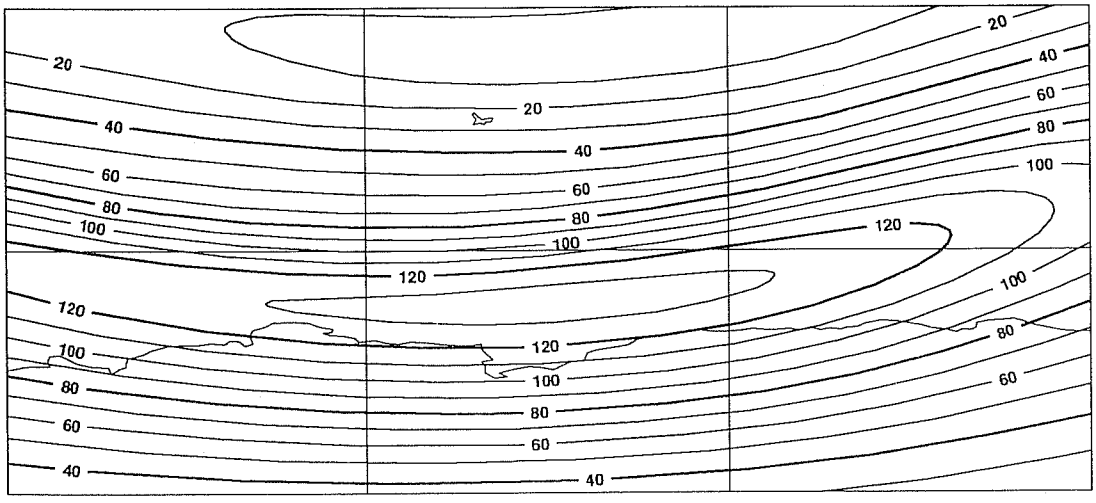

Fig. 14 T106L19 (upper) and T213L31 (middle) forecasts of wind speed (ms^{-1}) at four-day range valid 12UTC 1 August 1991, from the pre-operational trial of the higher resolution. The lower panel shows a T213L31 forecast with enhanced upper-level diffusion of divergence as used operationally.

140 ms^{-1} in the core of the jet. The corresponding trial T213L31 forecast (which then used a default timestep of 20 min, since reduced to 15 min for other reasons) is shown in the middle panel. This forecast used a semi-Lagrangian advection scheme which should have secured the integration from a purely advective computational instability. The noise seen in the middle panel of Fig. 14 was concentrated in the divergent component of the wind, and there was corresponding noise in the temperature field. This indicates a possible problem with the stability of the semi-implicit treatment of gravity-wave terms. The lower panel shows how the problem was circumvented by applying additional horizontal diffusion on the divergence field close to the top of the model when the 10 hPa wind exceeded 120 ms^{-1}.

5. GRAVITY-WAVE DRAG

It was noted earlier that a parametrization of gravity-wave drag (*Miller et al.*, 1989) was introduced operationally in July 1986. The scheme implemented initially gave relatively little drag in the lower troposphere and substantial drag in the stratosphere. Although of undoubted benefit to the tropospheric forecast, introduction of the scheme resulted in a tendency for substantial anomalies to develop in stratospheric PV fields over major mountain ranges (as will be illustrated), and diagnosis of the balance of the momentum budget provided clear evidence that the parametrized drag was too large in the stratosphere (*Klinker and Sardeshmukh*, 1992). Also, the scheme did not include a representation of high tropospheric drag associated with nonlinear gravity-wave resonance in high Froude number flows. Accordingly, a revised parametrization was introduced in May 1989 which gave more low-level drag, and less drag in the stratosphere. The parametrized component of the drag was also effectively reduced by the operational increase in horizontal resolution in September 1991, both because the subgridscale orographic variances became more localized and because the low-level flow tended to flow increasingly around rather than over mountain barriers.

A consequence of these changes is a dramatic change in stratospheric PV distributions. Recently, sequences of data assimilation and forecasts for spells in 1987 have been repeated with the current version of the forecasting system and T213L31 resolution. Fig. 15 compares the day-3 forecast of PV on the 475 K surface produced operationally from the analysis for 31 January 1987 with the corresponding forecast from the current, high resolution system. Both forecasts show the polar vortex to be displaced away from the pole and substantially distorted. The operational forecast also shows several other regions of high PV of which there is at most a vague indication in the rerun forecasts. The corresponding maps for two days later are shown in Fig. 16. The new forecast indicates a patch of high PV that has been detached from the main vortex. This can be seen also in the operational forecast, but without the benefit of the new forecast it would be difficult to distinguish it from the extensive band of high PV that has apparently been forced by the gravity-wave drag parametrization over the Asian and Rocky mountains.

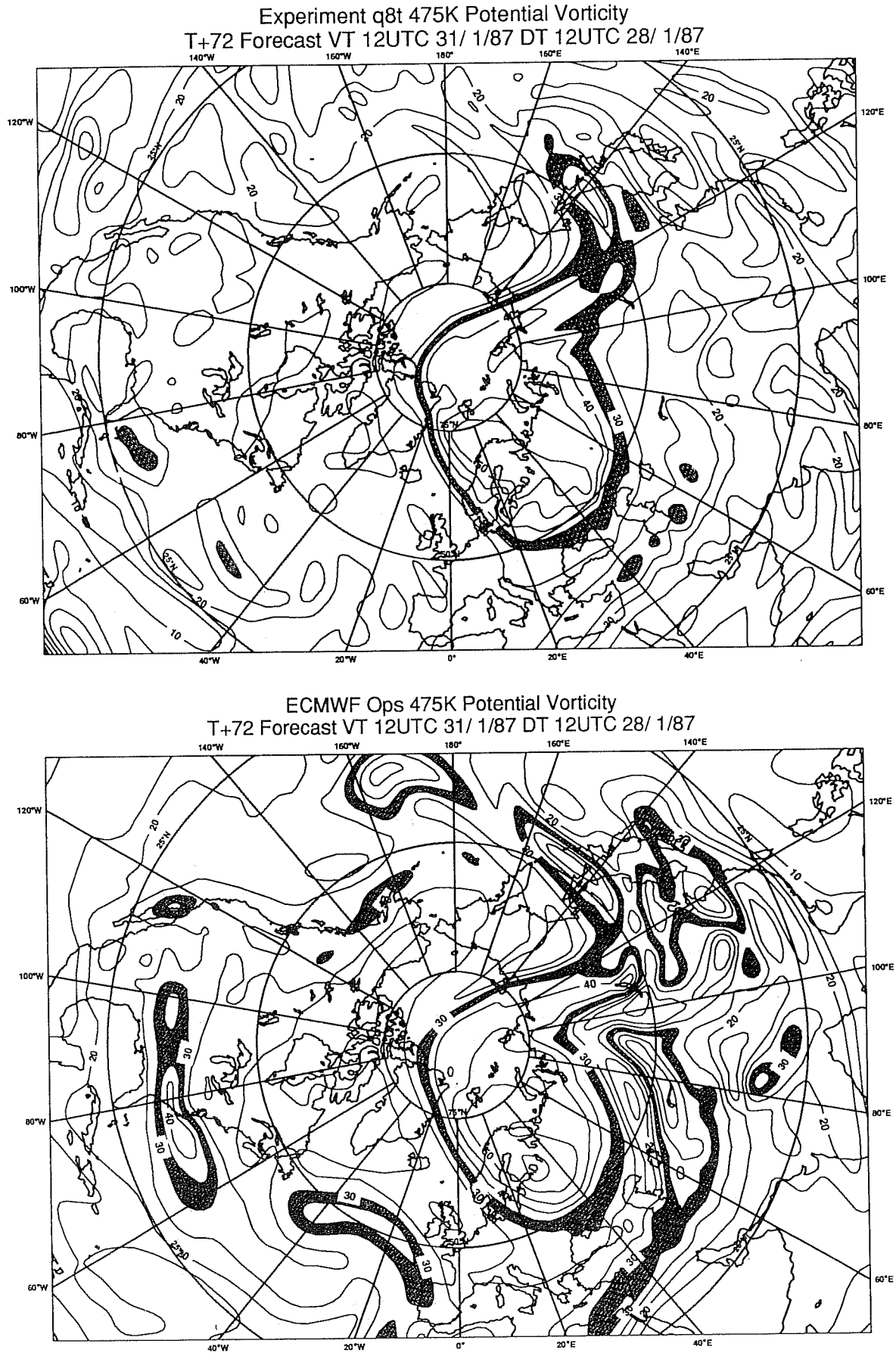

Fig. 15 Potential vorticity on the 475 K surface for day-3 forecasts verifying 12UTC 31 January 1987. The upper plot shows the result of a recent reanalysis and forecast using T213L31 resolution, and the lower plot shows the operational forecast produced in 1987.

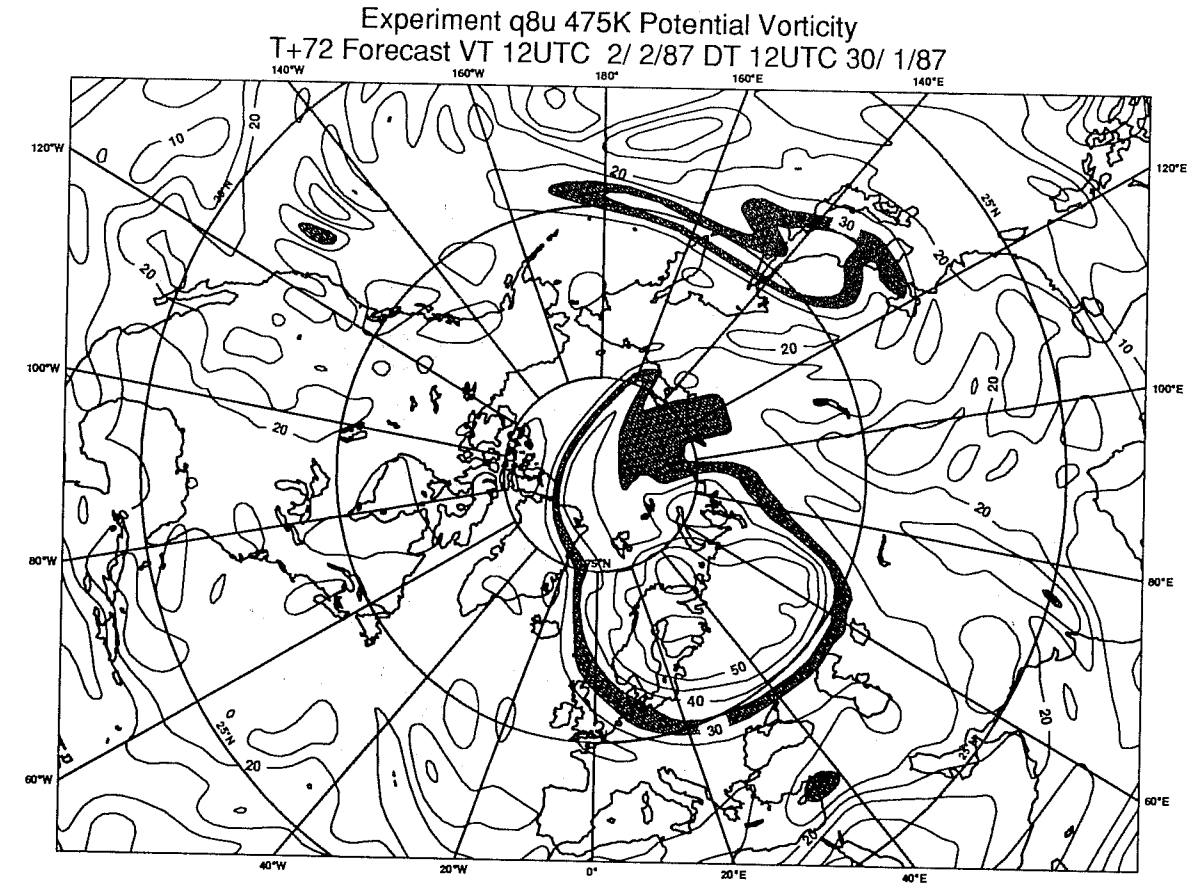

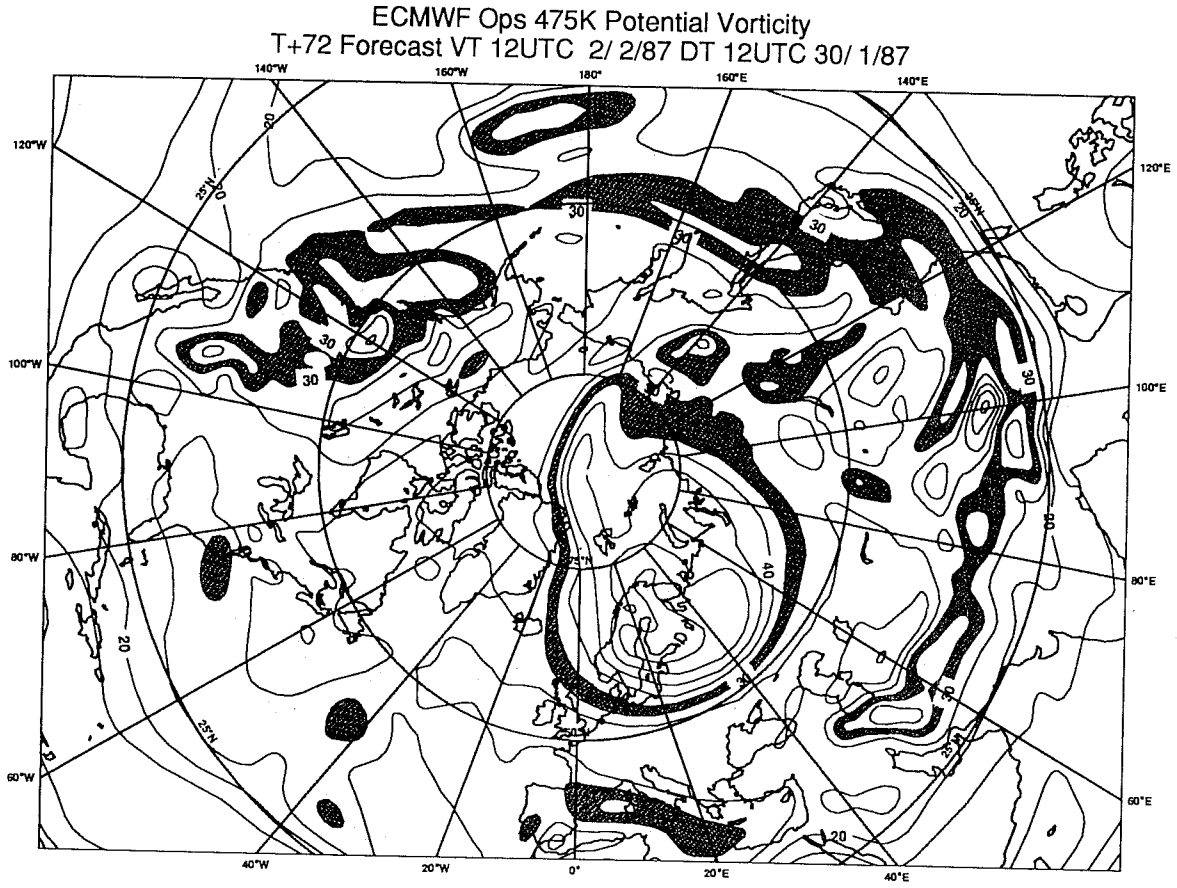

Fig. 16 As Fig. 16, but for 2 February 1987.

Although the parametrized gravity-wave drag diminishes with increasing resolution, the resolved gravity-wave activity increases. Fig. 17 shows vertical velocity at 100, 50 and 10 hPa from day-3 forecasts carried out at T106L19 and T213L31 resolution, plotted with a uniform contour interval for ω/p. The synoptic situation was one in which there was strong southwesterly flow in the troposphere incident upon the coastal range of British Columbia and the main ridge of the Rocky Mountains to the east. The increased amplitude and smaller scale of the induced vertical velocity pattern in the higher-resolution forecast can be seen clearly. Repeating the T213L31 forecast without the enhanced horizontal diffusion in the stratosphere results in an increase of amplitude by a factor of about two at 10 hPa. As discussed in the proceedings of the 1986 ECMWF Workshop on the Observation, Theory and Modelling of Orographic Effects, there are problems both in the accuracy of the explicit treatment of gravity waves that occur at scales close to the truncation limit and in knowing how to achieve the correct partition between parametrized and resolved gravity-wave effects.

6. SENSITIVITY TO NUMERICAL FORMULATION

Apart from the case of small-scale wave motion, sensitivity in the stratosphere to the numerical formulation of the model may be expected to be seen close to the tropopause, where there are rapid changes of gradient, and close to the top of the model, where vertical resolution is coarse. Two examples from recent work are presented here.

Sensitivity of model performance in the vicinity of the tropopause has been a concern to those developing semi-Lagrangian versions of their models (*Ritchie*, 1991; *Williamson and Olson*, 1994). The semi-Lagrangian version introduced operationally at ECMWF in September 1991 adopted a fully interpolating formulation (*Ritchie et al.*, 1994). When compared with the Eulerian version used previously, differences in mean thermal structure were indeed relatively large near the tropopause. The differences become more pronounced in extended range simulations to determine the model climate. Fig. 18 compares errors in zonal-mean temperature averaged for the December to February period from a set of 119-day T63L19 integrations from 1 November 1990. Each panel represents the result from just one simulation, but errors are sufficiently large, and similar in pattern to those seen repeatedly in 10-day forecast experiments, that the patterns are believed to be representative. The upper panel shows the result for the Eulerian advection scheme, and the middle panel the result for the semi-Lagrangian version. The latter gives a much lower cooling error near the polar tropopause, but a much larger error around the tropical tropopause. The lower panel shows results from the "vertically non-interpolating" semi-Lagrangian version currently used in operations (see again *Ritchie et al.*, 1994). The vertical component of the advection is Eulerian virtually everywhere with this version, and the error in zonal-mean temperature is very close to that from the purely Eulerian version.

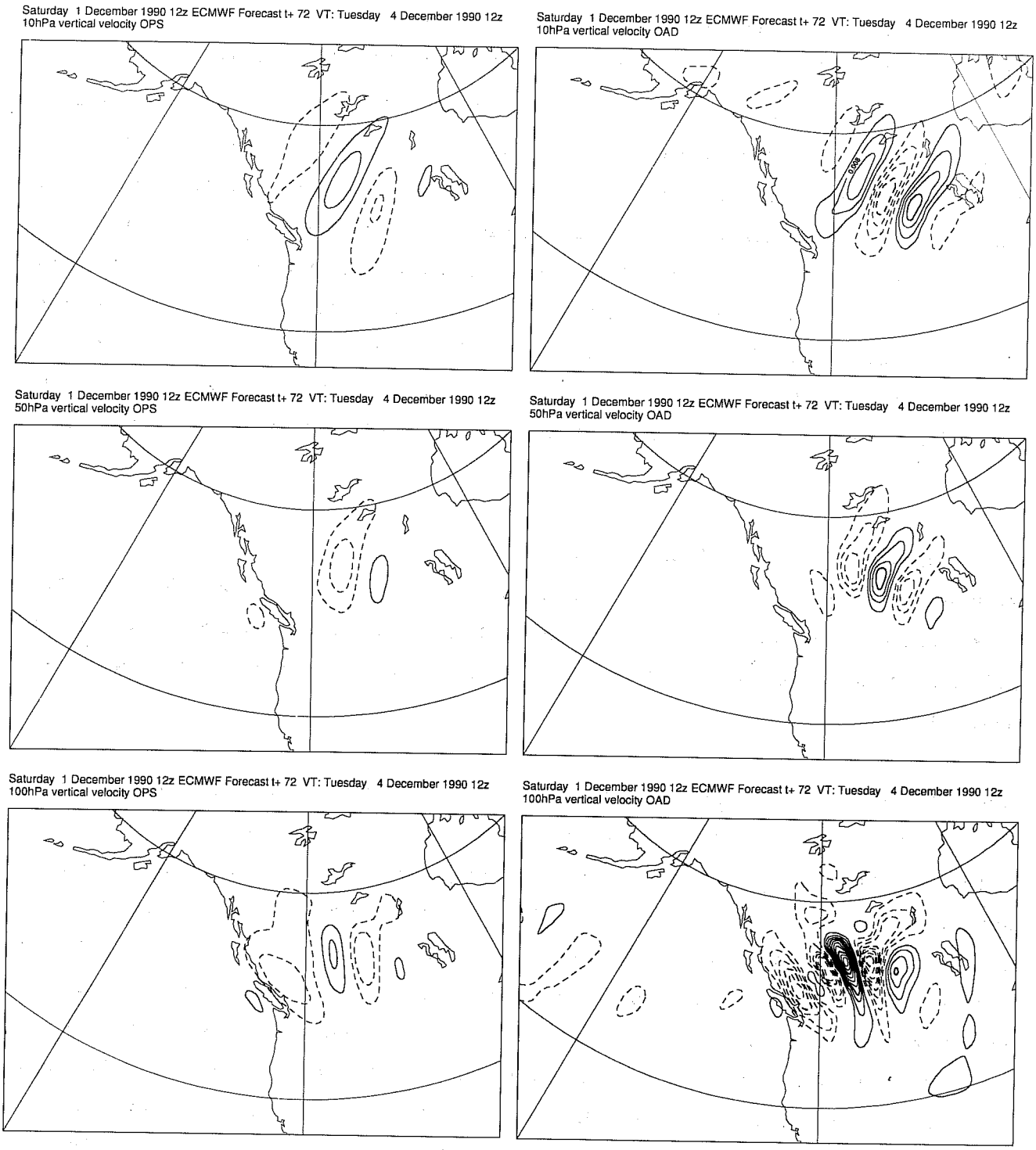

Fig. 17 Vertical velocity at 10 hPa (upper), 50 hPa (middle) and 100 hPa (lower) from T106L19 (left) and T213L31 (right) forecasts, for D+3 verifying 12UTC 4 December 1990. The contour interval is proportional to the pressure.

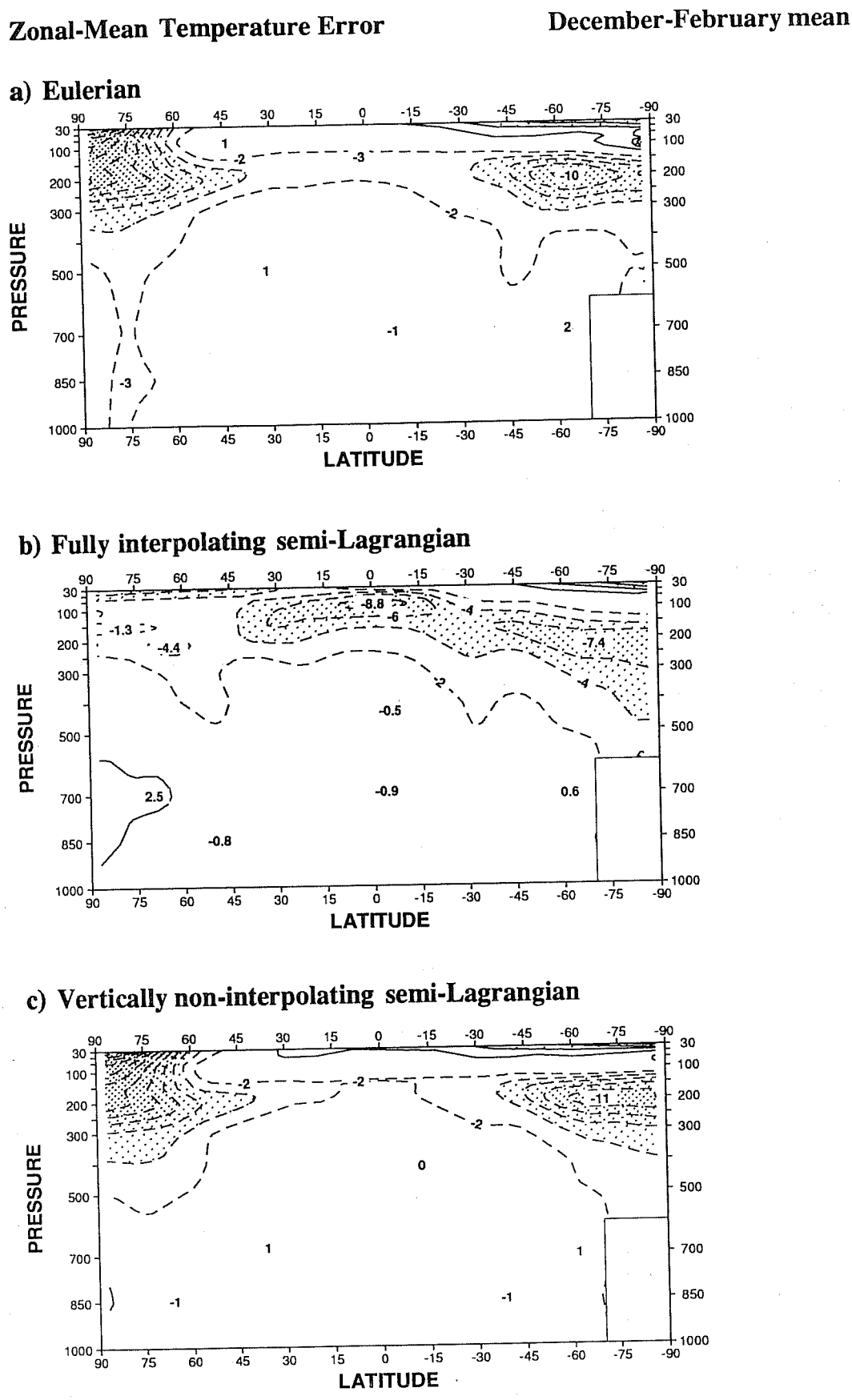

Fig. 18 Zonal-mean temperature errors from extended T63L19 simulations using Eulerian and semi-Lagrangian integration schemes. The contour interval is 2 K.

The second example is also one of sensitivity to the semi-Lagrangian formulation, and shows how this sensitivity can result in quite substantial analysis differences in the data-sparse tropical middle stratosphere. This example is another drawn from the data assimilation tests carried out for the period 7 to 27 January 1993. Mean differences in 12UTC wind analyses for this period are presented for the 10, 30 and 50 hPa levels in Fig. 19. The two analyses being compared differ only in the numerical scheme used in the assimilating (T106L31) model. One used the fully interpolating version of the semi-Lagrangian scheme and the other the vertically non-interpolating version, the latter being expected, as in the first example, to give results similar to those that would have been obtained had an assimilation been run with the conventional Eulerian version. At 30 hPa, wind differences reach of the order of 10 ms^{-1} close to the equator, and the zonal component predominates. Differences are generally smaller at 10 and 50 hPa, where they tend to be opposite in direction to those at 30 hPa. Differences can be seen to be rather more widespread at 10 hPa.

7. RESULTS OF USING HIGHER STRATOSPHERIC RESOLUTION

We have recently begun to reconsider the question of stratospheric resolution for the ECMWF model. The initial experiments have used a 38-level resolution in which the top full level is at 2.5 hPa, and the layer separation between 5 hPa and 80 hPa is reduced from 20 to 10 hPa. The location of levels is changed by at most a few hPa below about 300 hPa. Full-level pressures are given in Table 2, for levels higher than 350 hPa for a surface pressure of 1013.25 hPa, and higher than 250 hPa for a surface pressure of 500 hPa.

Number of levels	31	38	31	38
Full-level pressures		**2½**		**2½**
	10	10	10	10
		20		**20**
	30	30	30	30
		40		**40**
	50	50	50	50
		60		**60**
	70	70	70	70
		80		**80**
	90	91	90	90
		103		**101**
	111	116	110	113
	132	132	129	125
	156	150		**139**
	181	171	148	152
		194	166	167
	209	219	184	182
	238	247	201	197
	270	278	216	212
	304	310	231	227
	340	344	246	242
	p_s = 1013.25 hPa		**p_s = 500 hPa**	

Table 2 Upper full-level pressures, for surface pressures of 1013.25 and 500 hPa, for the 31- and 38-level vertical resolutions

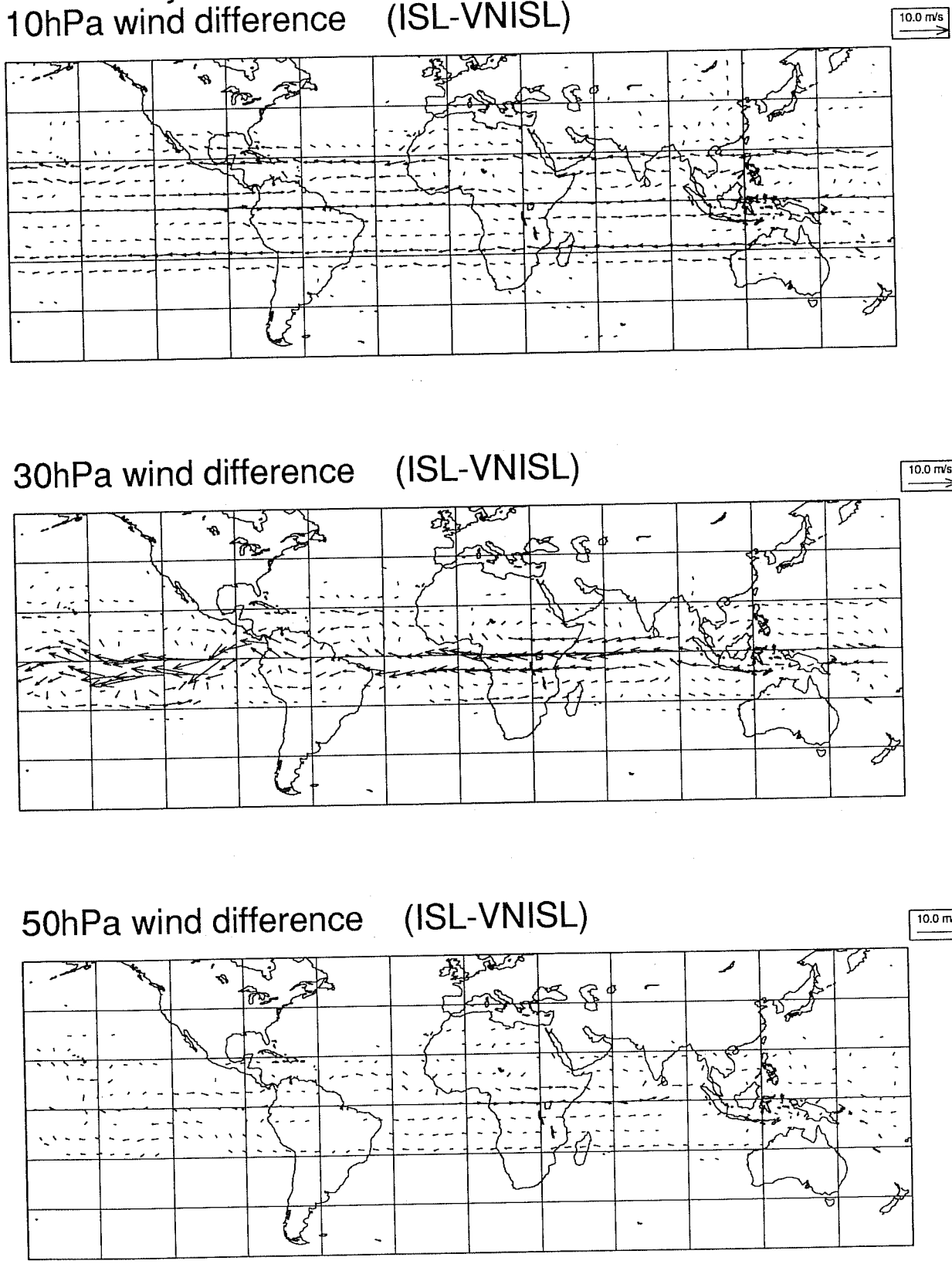

Fig. 19 Mean wind differences at 10, 30 and 50 hPa from data assimilations for the period 7 to 27 January 1993, using T106L31 resolution and fully interpolating (ISL) and vertically non-interpolating (VNISL) semi-Lagrangian integration schemes.

A set of seven forecasts has been carried out from 12UTC analyses for each day from 13 to 19 January 1992 using T213L31 and T213L38 resolutions. The trial 31-level analyses referred to in section 4 were used, with interpolation and extrapolation to produce the 38-level data sets. The period chosen was from within that of the European Arctic Stratospheric Ozone Experiment (EASOE), and was one for which the stratospheric vortex became considerably distorted within the range of the forecasts. This has been discussed by Plumb at this workshop. Also, *Carver et al.* (1994) have examined sensitivity to stratospheric resolution in forecasts from 17 January 1992 using the UGAMP GCM, which was derived from an earlier version of the ECMWF model.

Synoptic assessment of the stratospheric forecasts produced by the 38- and 31-level versions of the model indicates an obvious superiority of the 38-level forecasts. This can be clearly seen in the day-7 50 hPa and 10 hPa forecasts from 17 and 18 January presented in Figs. 20 and 21. At 50 hPa the trough in the sector from 30^0E to 90^0E is treated much better in the higher resolution forecasts, and at 10 hPa the location of the Aleutian High and shape and orientation of the vortex are markedly superior. Maps of PV on the 475 K surface (Figs. 22 and 23) show generally sharper gradients for the 38-level forecasts, and in particular more pronounced intrusions of air from outside the vortex. This is as found also by *Carver et al.* (1994), and is in agreement with observations and contour advection calculations presented here by Plumb.

The superiority of the 38-level stratospheric forecasts is also evident in objective verification of the sample of seven cases. RMS height and wind verifications for the 10 and 30 hPa levels are presented in Fig. 24.

Height verifications for lower levels are presented in Fig. 25. The 38-level forecasts show up as better at 50 hPa, as at 30 and 10 hPa, apart from the period from day 4 to day 6. A small benefit of the better stratospheric representation can also be seen at 200 hPa, starting at about day 2, and a slight advantage can be seen at lower, tropospheric levels. The impact of the stratospheric change becomes just discernible at about day 3 at 500 hPa and day 5 at 1000 hPa.

It would probably be misleading to attempt to draw specific conclusions on the basis of these first experiments from one specially chosen period with no assimilation carried out for the higher stratospheric resolution. Results are nevertheless encouraging, and tests in data assimilation and extended-range simulation are planned.

Acknowledgements

The reanalysis group at ECMWF are thanked for making available the results of their preparatory experimentation, as are those staff members of ECMWF who contributed to the work summarized here.

ECMWF Analysis VT: Thursday 23 January 1992 12z
50hPa height

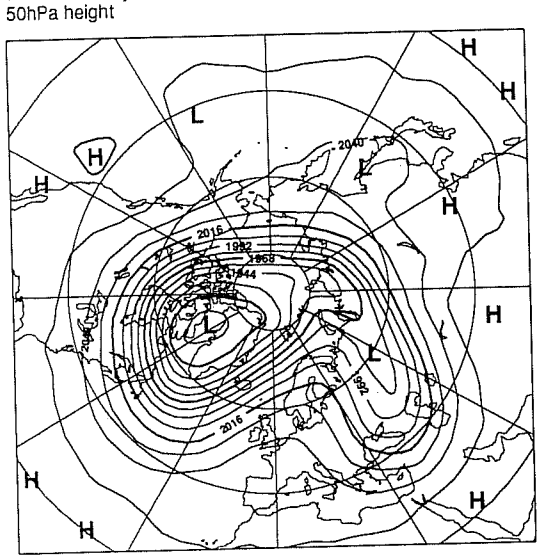

ECMWF Analysis VT: Thursday 23 January 1992 12z
10hPa height

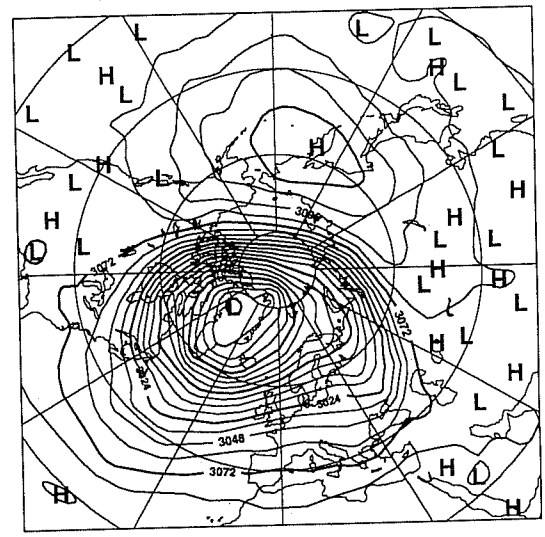

Thursday 16 January 1992 12z ECMWF Forecast t+168 VT: Thursday 23 January 1992 12z
50hPa height t213 l38

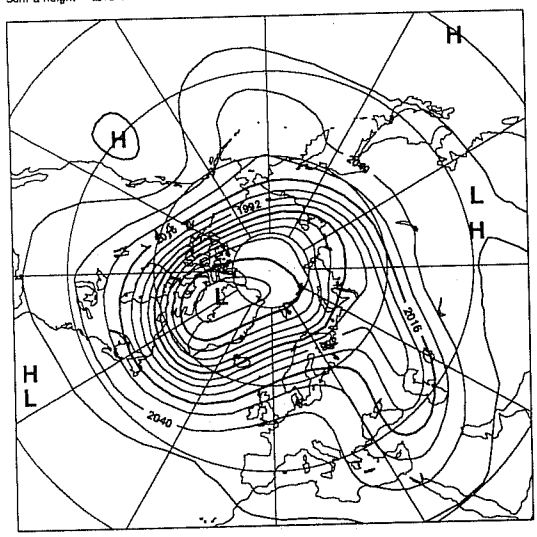

Thursday 16 January 1992 12z ECMWF Forecast t+168 VT: Thursday 23 January 1992 12z
10hPa height t213 l38

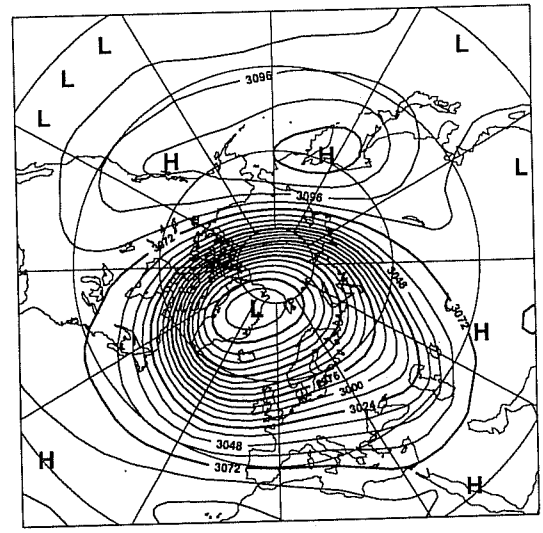

Thursday 16 January 1992 12z ECMWF Forecast t+168 VT: Thursday 23 January 1992 12z
50hPa height t213 l31

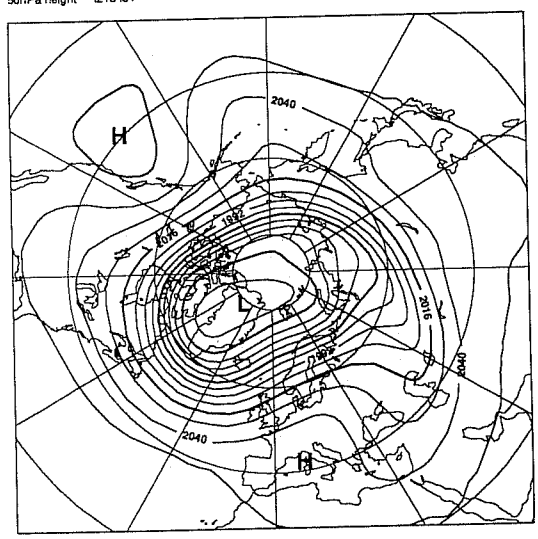

Thursday 16 January 1992 12z ECMWF Forecast t+168 VT: Thursday 23 January 1992 12z
10hPa height t213 l31

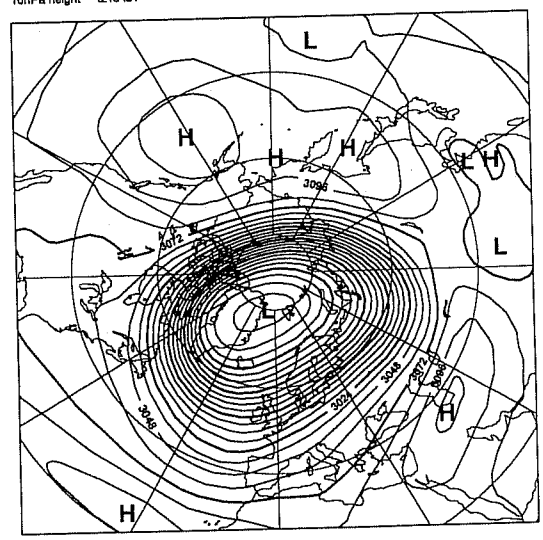

Fig. 20 . 50 hPa (left) and 10 hPa (right) height maps (contour interval 12 dam) for 12UTC 23 January 1992 for:
Upper: Verifying analysis
Middle: Day-7 forecast from T213L38
Lower: Day-7 forecast from T213L31

ECMWF Analysis VT: Friday 24 January 1992 12z
50hPa height

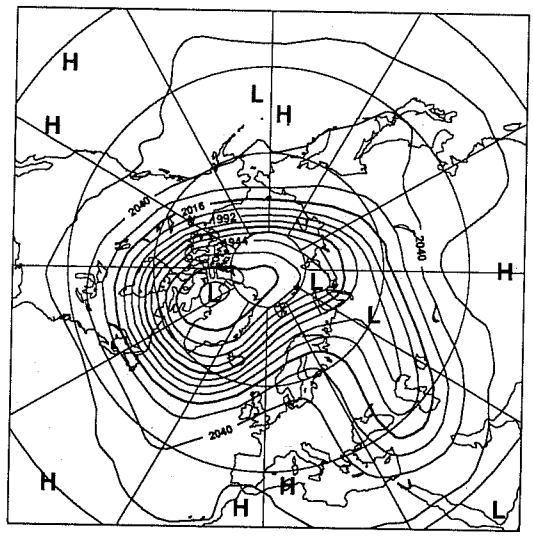

ECMWF Analysis VT: Friday 24 January 1992 12z
10hPa height

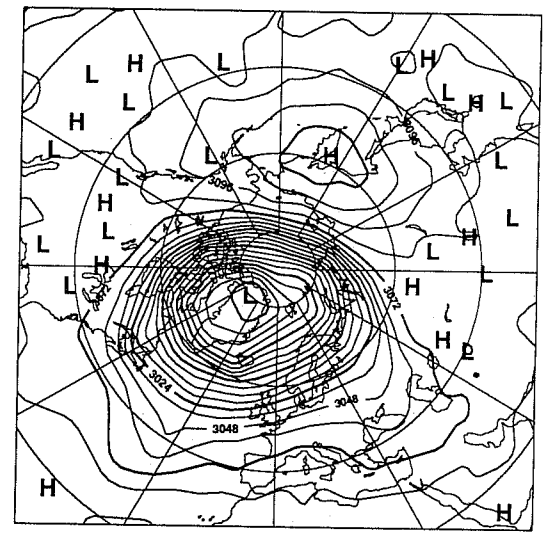

Friday 17 January 1992 12z ECMWF Forecast t+168 VT: Friday 24 January 1992 12z
50hPa height t213 l38

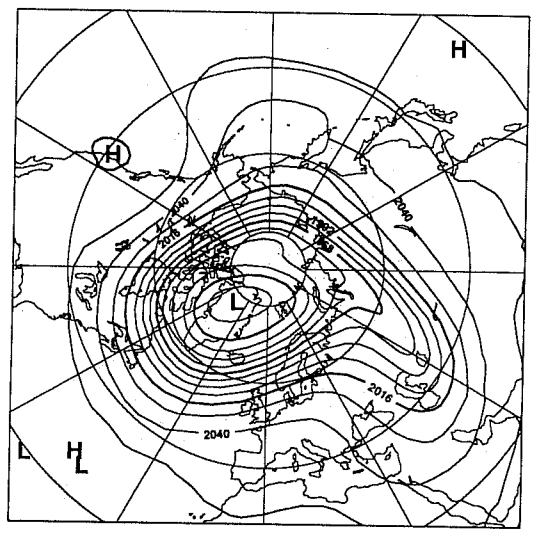

Friday 17 January 1992 12z ECMWF Forecast t+168 VT: Friday 24 January 1992 12z
10hPa height t213 l38

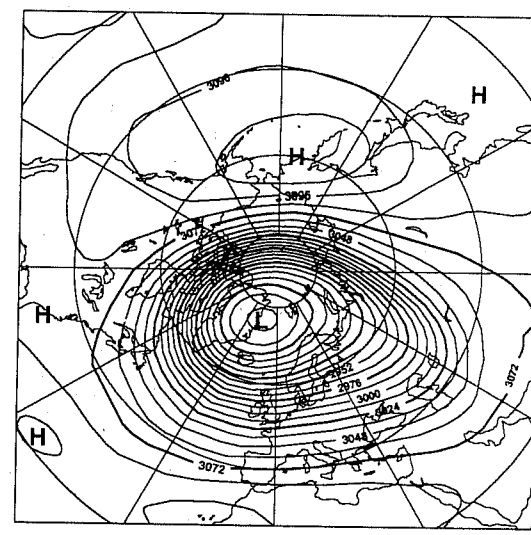

Friday 17 January 1992 12z ECMWF Forecast t+168 VT: Friday 24 January 1992 12z
50hPa height t213 l31

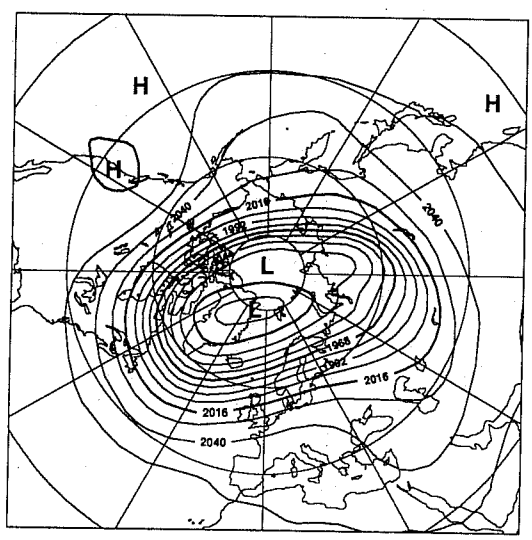

Friday 17 January 1992 12z ECMWF Forecast t+168 VT: Friday 24 January 1992 12z
10hPa height t213 l31

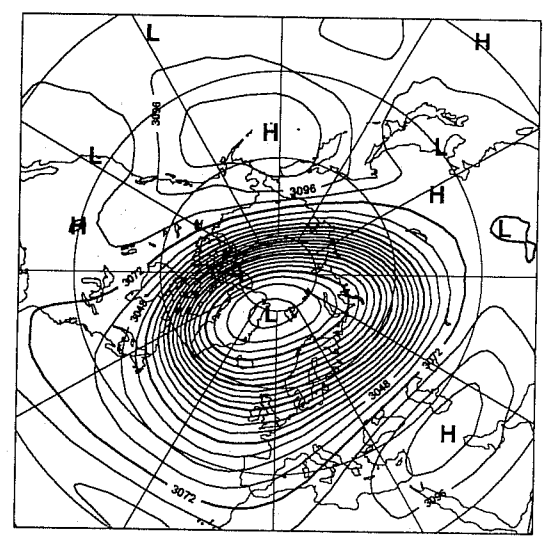

Fig. 21 As Fig. 21, but for 24 January 1992.

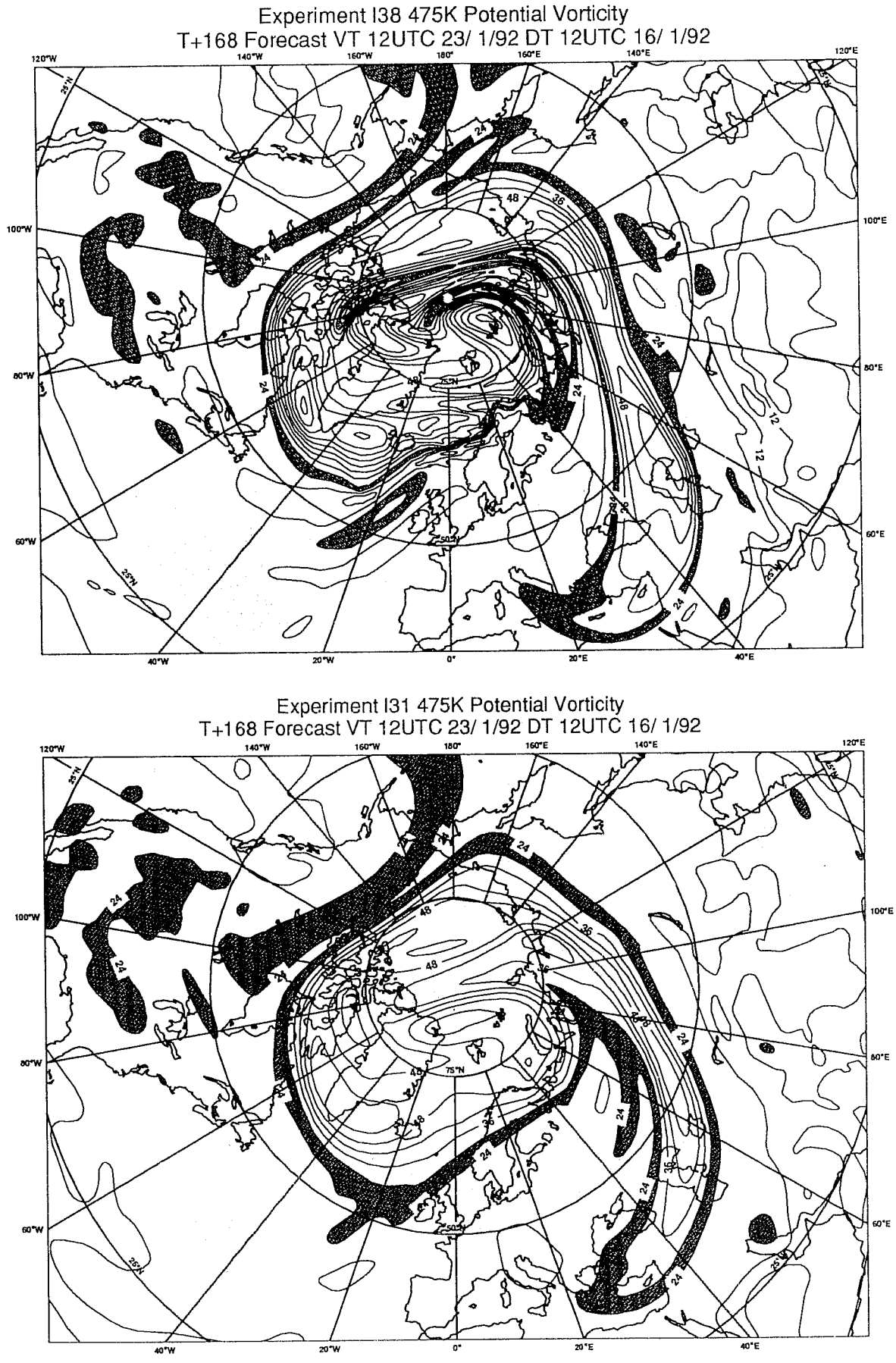

Fig. 22 Potential vorticity on the 475 K surface from day-7 forecasts valid 12UTC 23 January 1992 using T213L38 resolution (upper) and T213L31 resolution (lower).

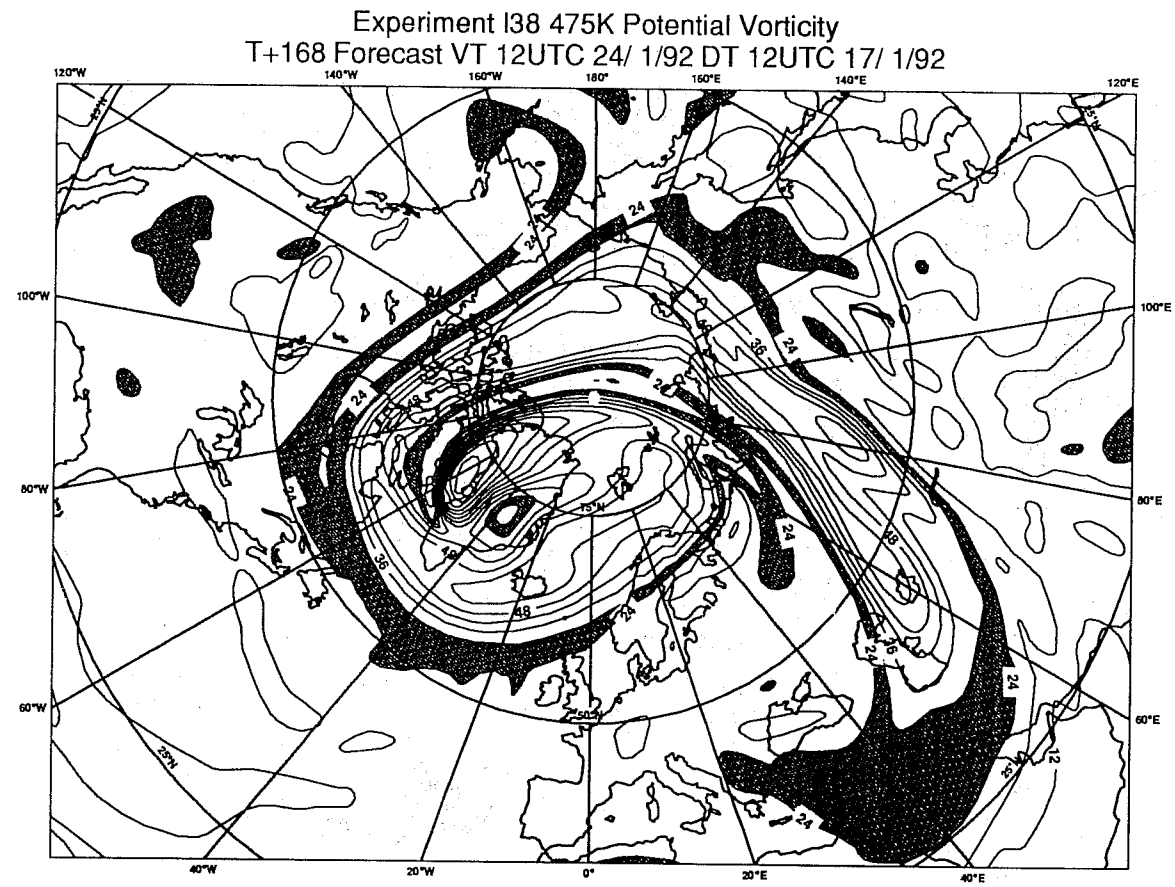

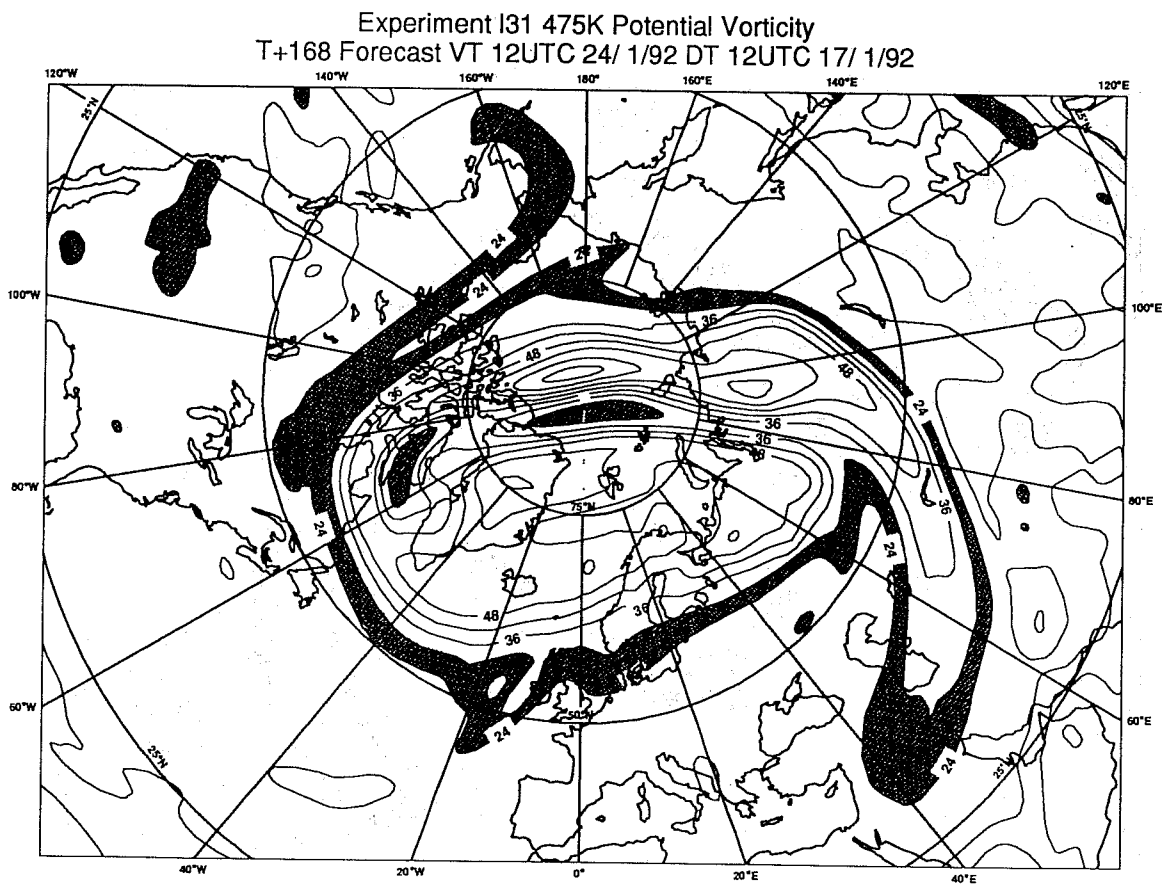

Fig. 23 As Fig. 23, but for 24 January 1992.

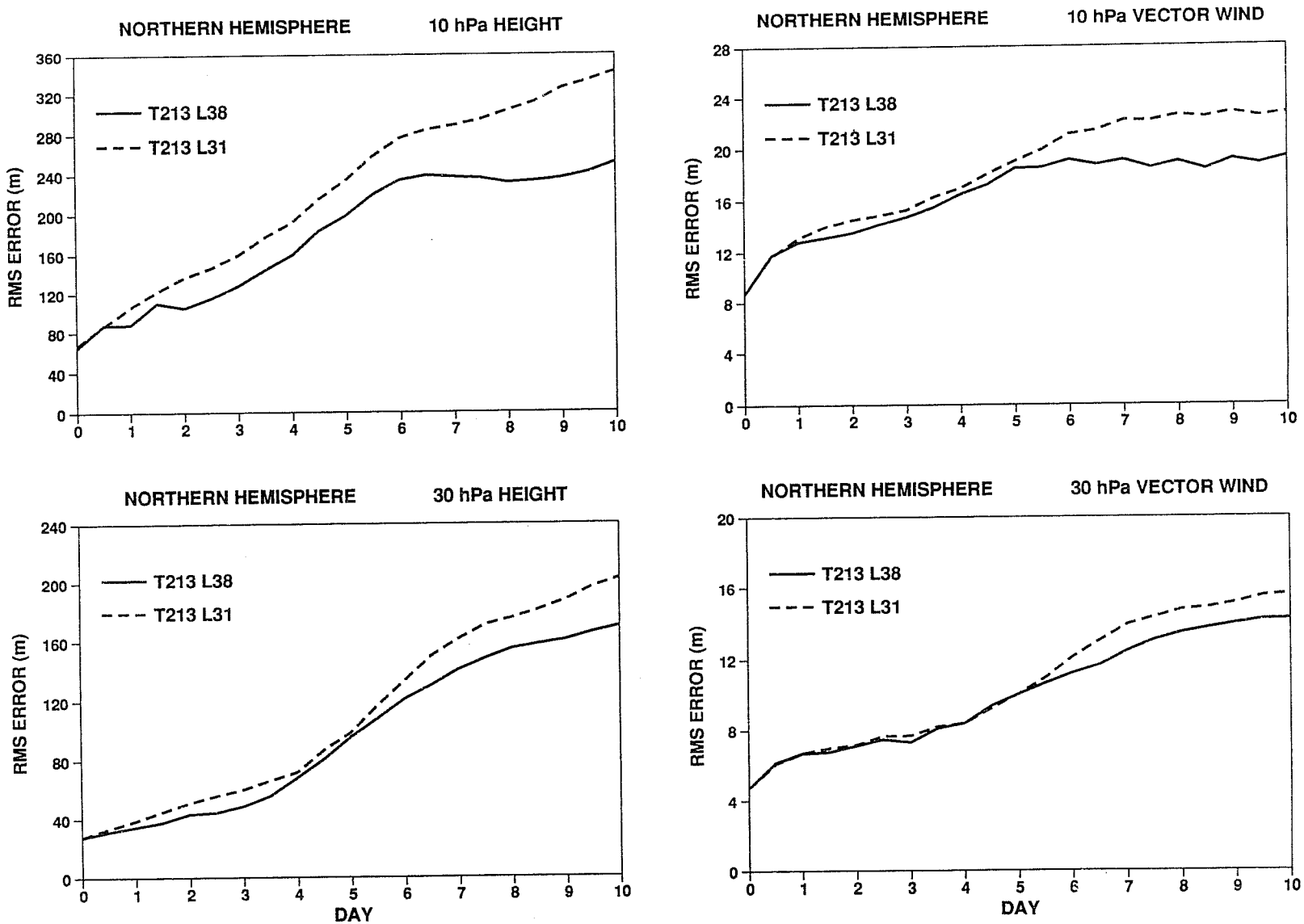

Fig. 24 Root mean square errors of the 10 hPa and 30 hPa heights and vector winds, computed over the extratropical Northern Hemisphere, and averaged over forecasts from 12UTC, 13 to 19 January 1992.

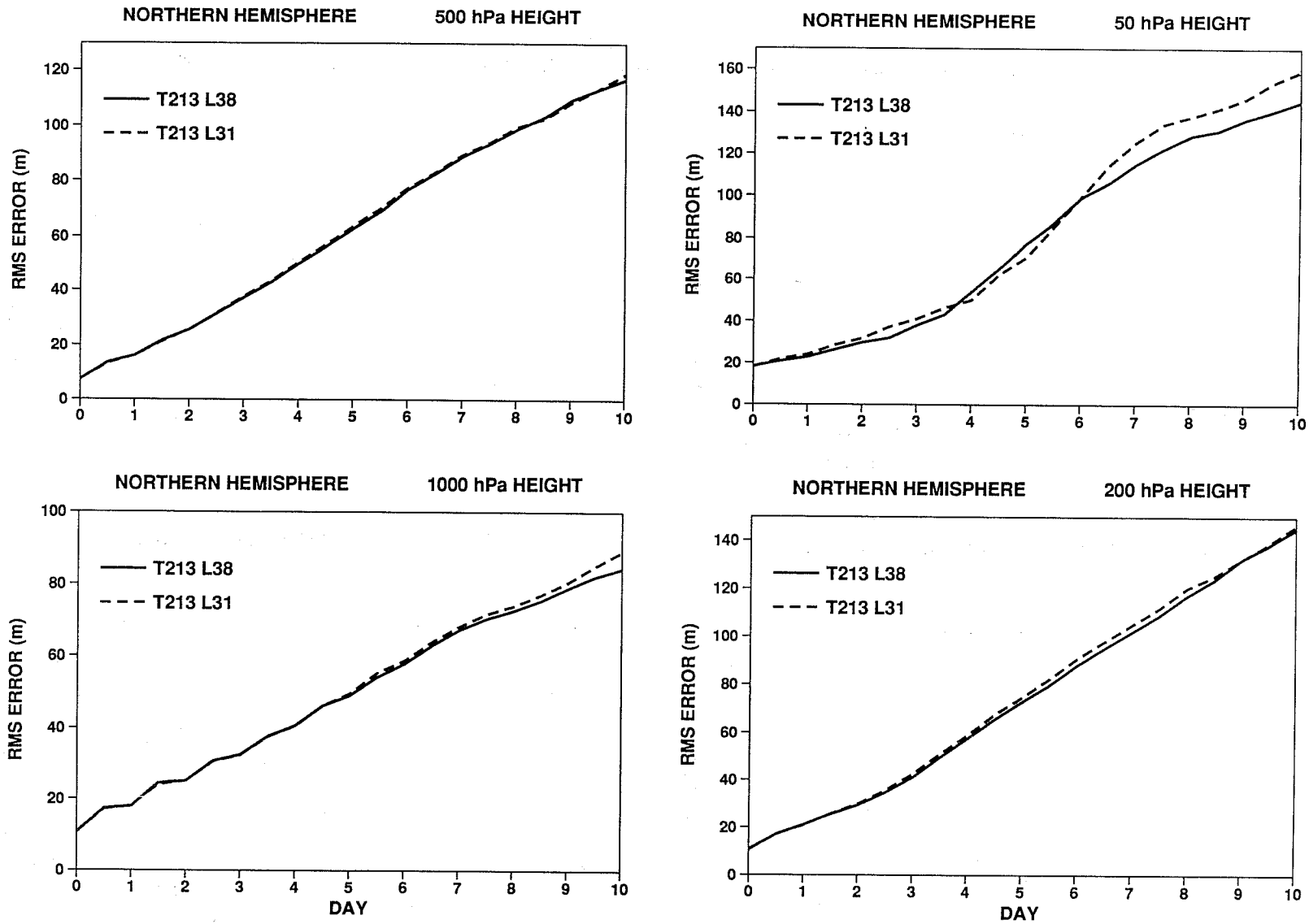

Fig. 25 Root mean square errors of the 50 hPa, 200 hPa, 500 hPa and 1000 hPa heights, computed over the extratropical Northern Hemisphere, and averaged over forecasts from 12UTC, 13 to 19 January 1992.

References

Boville, B.A., 1984: The influence of the polar night jet on the tropospheric circulation in a GCM. J. Atmos. Sci., 41, 1132-1142.

Carver, G.D., W.A. Norton and J.A. Pyle, 1994: Forecasting the disturbed stratospheric arctic vortex of January 1992. To appear in Geophys. Res. Lett..

Fels, S.B., J.D. Mahlman, M.D. Schwarzkopf and R.W. Sinclair, 1980: Stratospheric sensitivity to perturbations in ozone and carbon dioxide: Radiative and dynamical response. J. Atmos. Sci., 37, 2265-2297.

Klinker, E. and P.D. Sardeshmukh, 1992: The diagnosis of mechanical dissipation in the atmosphere from large-scale balance requirements. J. Atmos. Sci., 49, 608-627.

Miller, M.J., T.N. Palmer and R. Swinbank, 1989: Parametrization and influence of subgridscale orography in general circulation and numerical weather prediction models. Meteor. Atmos. Phys., 40, 84-109.

Ritchie, H., 1991: Application of the semi-Lagrangian method to a multi-level spectral primitive-equations model. Quart. J. Roy. Meteor. Soc., 117, 91-106.

Ritchie, H., C. Temperton, A. Simmons, M. Hortal, D. Dent and M. Hamrud, 1994: Implementation of the semi-Lagrangian method in a high resolution version of the ECMWF forecast model. In preparation.

Schlesinger, M.E. and Y. Mintz, 1979: Numerical simulation of ozone production, transport and distribution with a global atmospheric general circulation model. J. Atmos. Sci., 36, 1325-1361.

Simmons, A.J., 1987: Orography and the development of the ECMWF forecast model. ECMWF Seminar on Observation, Theory and Modelling of Orographic Effects, Vol. 2, 129-163.

Simmons, A.J. and D.M. Burridge, 1981: An energy and angular-momentum conserving vertical finite-difference scheme and hybrid vertical coordinates. Mon. Wea. Rev., 109, 758-766.

Simmons, A.J. and R. Strüfing, 1983: Numerical forecasts of stratospheric warming events using a model with a hybrid vertical coordinate. Quart. J. Roy. Meteor. Soc., 109, 81-111.

Simmons, A.J., D.M. Burridge, M. Jarraud, C. Girard and W. Wergen, 1989: The ECMWF medium-range prediction models: Development of the numerical formulations and the impact of increased resolution. Meteor. Atmos. Phys., 40, 28-60.

Tuck, A.F., T. Davies, S.J. Hovde, M. Noguer-Alba, D.W. Fahey, S.R. Kawa, K.K. Kelly, D.M. Murphy, M.H. Proffitt, J.J. Margitan, M. Loewenstein, J.R. Podolske, S.E. Strahan and K.R. Chan, 1992: Polar stratospheric cloud processed air and potential vorticity in the Northern Hemisphere lower stratosphere at mid-latitudes during winter. J. Geophys. Res., 97, 7883-7904.

Williamson, D.L. and J.G. Olson, 1994: Climate simulations with a semi-Lagrangian version of the NCAR CCM2. Submitted to Mon. Wea. Rev.